CONSTANT DIAMETER AIR INJECTOR

by

Henry Joseph Tucker

Thesis submitted in partial fulfilment
of the requirements for the degree of
Master of Engineering

Department of Mechanical Engineering
McGill University
Montreal

August 1955

SUMMARY

A method is given for applying one-dimensional analysis to an injector with constant diameter mixing. A review is made of the theory for the turbulent mixing of air streams. Some of the difficulties of applying this theory to injectors are considered.

An outline of experimental work is given for a simple air injector with constant diameter mixing at low temperatures. In this injector a single convergent type primary nozzle was used operating at higher than critical pressure ratios. The diameter of the mixing tube was varied to give diameter ratios of mixing tube to primary nozzle of 2.2 to 5.7.

In this injector the ratio of secondary to primary mass flow varied from 0 to 4. The maximum static pressure rise in the mixing tube was about one atmosphere.

Graphs are presented which compare experimental results with those predicted from one-dimensional analysis. Curves are presented for the design of injectors for the range of variables investigated.

The static pressures along the mixing tube were observed in order to determine the lengths required for mixing. A complete set of pressure profile curves is presented, and the relation of the mixing length to the other variables given in graphical form.

ACKNOWLEDGEMENTS

The author wishes to express his sincere thanks to Professor D.L. Mordell who directed this research and to R.W. Foster-Pegg for his help and suggestions throughout the course of the experiment.

The staff of the Gas Dynamics Laboratory gave the author invaluable assistance in setting up the apparatus. The calibration of pressure gauges was done by J. Kelly, machining of the nozzles and orifice plates by W. Trudeau, photography by D. Turczeniuk and C. Farra welded the mixing tubes. Their assistance is much appreciated.

Thanks is due to the Department of Mines for the loan of manometers and a metering tank which were used for the experiment, and also to the Defence Research Board who gave financial aid for setting up the experimental apparatus.

The generous help of Jeannine Lacroix is acknowledged for typing the thesis and of Audrey Tucker who performed calculations, plotted graphs and helped to correlate data.

TABLE OF CONTENTS

LIST OF ILLUSTRATIONS AND GRAPHS

ILLUSTRATIONS PAGE

GRAPHS

TABLE OF NOMENCLATURE

SUBSCRIPTS

1 Primary jet in plane of nozzle exit.

2 Secondary jet at throat of nozzle.

3 Section of mixing tube where pressure recovery is maximum.

e Space before secondary nozzle throat.

m Mean value.

o Space before primary nozzle.

NOTATIONS

A Sectional area.

Cp Specific heat at constant pressure.

D Diameter.

g 32.17 acceleration of gravity (ft/sec^2).

k Constant.

k' Constant.

L Length required for mixing of primary and secondary fluids.

ℓ Mixing length in turbulent flow.

M Mass flow of air.

P Total pressure.

p Static pressure.

R Constant.

T Total temperature.

t Static temperature.

u	Velocity.
u'	Deviation from average velocity.
v	Velocity.
v'	Deviation from average velocity.
X	Distance from primary nozzle to throat of secondary nozzle.
y	Distance along axis.
γ	Ratio of specific heats Cp/Cv.
ϵ	Apparent viscosity.
μ	Viscosity.
ρ	Fluid density.
τ	Viscous shear stress.
τ'	Apparent shear stress.

CHAPTER I

INTRODUCTION

The injector is essentially a form of pump. A primary or actuating fluid flowing at a high velocity from a nozzle is allowed to mix with and transfer its momentum to a second fluid, called the secondary or induced fluid. By this action the secondary fluid may be made to flow at increased pressure.

Commercially, injectors have many applications. They are used for deep well and ash handling pumps, for boiler water feeding using steam as the primary fluid and also as a source of inducing draught in steam locomotives. Because of the complete absence of moving metal parts they are very reliable. This together with their inexpensive and simple construction makes them competitive with other forms of pumps even though the mechanical efficiency may be less.

Injectors are finding many new applications. With the advent of high power turbo jets the injector problem has received considerable attention as a means of utilizing tail pipe burning for thrust augmentation, or for supplying additional air for engine cooling. The injector seems promising for this service because of its simple construction and low weight. It has also been considered as a pump for removing boundary-layer air from aircraft wings and fuselage surfaces.

An application of the injector with which the author has been directly connected was to meter and feed coal to the furnace of the McGill experimental coal burning gas turbine. In this case the primary fluid was air which was bled from the compressor outlet, and the secondary medium consisted of fine coal particles about 90% being of less than 200 mesh in size. This feed system was used for about 200 hours of engine running at low power conditions. At high power running conditions with high furnace pressure it was found that the particular injector used could not pump sufficient coal against the increased pressure and gave an unsteady coal feed. In future tests the coal will be metered by other means and the injector will be used solely to convey the metered coal to the furnace.

No experimental results could be found for an injector pump for solid particles. Even when both primary and secondary fluids are air the data available is meagre and limited to a small range of variables. It was therefore thought logical that before proceeding with the more complicated case where the secondary medium was solid particles, to investigate the case of the secondary fluid being air and compare the performance with that predicted from the one-dimensional analysis. This thesis deals with this phase of the investigation.

A simple air injector was set up for the experiment. It was decided to use a constant diameter mixing section since one-dimensional treatment could be applied to this form. This injector was of the annular type with the primary air nozzle located centrally. Complications such as end diffusers were not used because it was thought that this was another problem which could be investigated separately.

CHAPTER II

THEORY

I - One-Dimensional Analysis

The performance of the injector may be obtained by treating the flow as "one-dimensional"; that is, a flow in which the velocity, the pressure and the temperature of the fluid are assumed to be constant over any given cross section. Although this supplies no information for the region where the primary and secondary fluids mix, it gives a way of calculating the overall performance which agrees fairly well with that obtained from actual tests, as will be shown from the results of the experiment. The application of one-dimensional analysis to the constant diameter injector will now be given.

In many flow processes the important flow variables defined by the conservation laws and the equation of state may be combined into a set of related dimensionless quantities: $\frac{u}{\sqrt{gRT}}$ the velocity parameter, $\frac{PA}{M\sqrt{gRT}}$ the total pressure parameter, $\frac{pA}{M\sqrt{gRT}}$ the static pressure parameter and $\frac{u}{\sqrt{gRT}} + \frac{pA}{M\sqrt{gRT}}$ the total momentum parameter. Other dimensionless parameters may be used but the above are chosen because they contain the mass flow M, the total temperature T, and the total pressure P, which may be considered to remain constant in many flow processes. These parameters are related to the pressure ratio $\frac{P}{p}$ by a group of equations for adiabatic flow processes which are given in Appendix I. In Ref. 17 curves are plotted from these equations which relate the above parameters and facilitates the handling of flow problems.

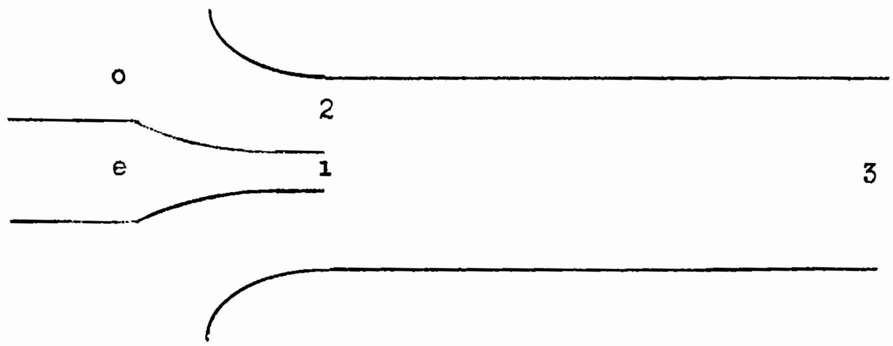

Fig. 1. Cross Section of Injector.

A diagrammatic sketch of the cross section of the injector is shown in Fig. 1. Primary air flows from the reservoir "e" and issues from the exit of the primary nozzle shown as "1" in the diagram. The secondary air flows from region "o" through the annular space between primary nozzle and mixing tube shown as "2". The two flows come together and mix with transfer of mass and momentum and leave the mixing tube at section "3".

For the one-dimensional treatment of the injector the following assumptions are made:

(1) Uniform velocity and pressure at "1" the exit of the primary nozzle, and also at "2" the throat of the

secondary nozzle.

(2) Complete mixing of air streams and so uniform velocity and pressure at section "3" the exit of the mixing tube.

(3) No heat transfer across the boundary of the mixing tube.

(4) Values of Cp and γ for both fluids are constant and equal to 0.24 and 1.4 respectively.

(5) No friction losses in nozzles or mixing tube.

Considering the conditions at the inlet and outlet of the mixing section and applying the law of conservation of momentum, the law of conservation of mass and assuming (5) no losses in the mixing tube, the following equation is obtained.

$$M_1 u_1 + p_1 A_1 + M_2 u_2 + p_2 A_2 = (M_1 + M_2)\, u_3 + p_3\, (A_1 + A_2) \quad \ldots (1)$$

This is the momentum equation for the constant diameter injector.

The method used to calculate the performance of the injector will now be given. Consider first the primary converging nozzle. If the pressure ratio p_e/p_2 is less than the critical value, then p_1 will remain equal to p_2 at all times. If the ratio p_e/p_2 is greater than the critical value the nozzle becomes chocked, the pressure at "1" will then increase as p_e is increased, the ratio p_e/p_2 remaining constant at the critical value and the jet will expand beyond section "1" of the nozzle.

In a convergent nozzle operating above the critical pressure ratio the static pressure parameter $\dfrac{p_1 A_1}{M_1 \sqrt{gRT_e}}$ remains constant and neglecting the nozzle losses

$$M_1 = k_1 A_1 \frac{p_e}{\sqrt{T_e}} \quad \dots\dots\dots\dots\dots\dots\dots\dots\dots\dots (2)$$

For a constant pressure ratio the momentum parameter also remains constant and the momentum can be calculated by the formula

$$M_1 u_1 + p_1 A_1 = k_1' p_e A_1 \quad \dots\dots\dots\dots\dots\dots\dots\dots\dots (3)$$

Thus for a given converging nozzle the mass flow and momentum can be calculated if A_1, p_e and T_e are known.

In the calculations of the secondary mass flows and momenta the following procedure was followed. A static pressure was assumed for section "2" the throat of the secondary nozzle. The ratio p_o/p_2 can be calculated which fixes all the other parameters at this section. The mass flows and the momenta can then be calculated from the adiabatic flow equations given in the appendix or more conveniently from parameter curves such as plotted in Ref. 17.

By adding the mass flows and momenta at "1" and "2", the mass flows and momentum at section "3" can be found. The momentum parameter can then be calculated and all the other parameters found from curves Ref. 17. This was the method used to calculate the theoretical curves given in Figs. 15, 16, 17 and 18 of the report.

As already mentioned this method of analysis does not concern the very essential mixing process which occurs between sections "1" and "3". Therefore the present knowledge of turbulent mixing of streams will be reviewed.

II Turbulent Theory

If two streams of fluid of different velocities and properties unite after passing some boundary as shown in Fig. 2, identations increase rapidly in size. This results in the surface of discontinuity breaking down into a large number of eddies or vortices which are usually irregular. Because of fluctuations in the flow the surface at the boundary between the two fluids may take on a slightly wavy foam as shown in Fig. 3. If a system of co-ordinates is taken which move along with a velocity equal to the mean velocity of the two streams then the wave crests and troughs will remain at rest. With respect to this system of co-ordinates the upper fluid is flowing towards the right while the lower fluid is flowing towards the left. Applying Bernoulli's theorem will lead to

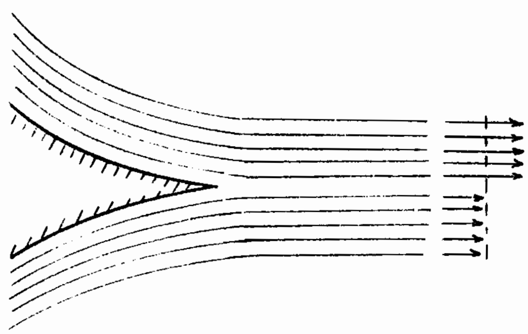

Fig.2. Two Streams of Fluid Flowing Together.

the conclusion that the motion being assumed steady there is an excess of pressure at the crests of each fluid and a defect of pressure at the troughs. This distribution of pressure indicates that the motion cannot be steady, for the fluid in the region of excess pressure will tend to move into the neighbouring region where there is reduced pressure. This causes the undulations to become more marked, resulting in the surface of discontinuity breaking down into separate eddies. This concept is given by Prandtl (Ref. 12).

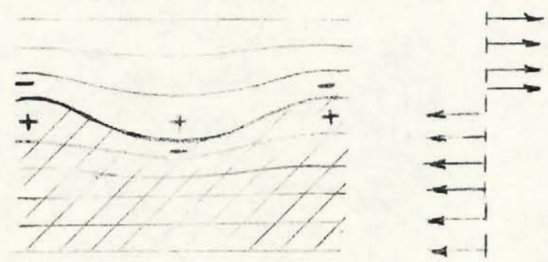

Fig. 3. Fluid Streams with Undulations.

The final state usually consists of an irregular medley of large and small eddies as shown in Fig. 4. Thus it can be seen that mixing of two fluid streams is subject to considerable and usually irregular fluctuations. However the time average of the velocities at different points taken

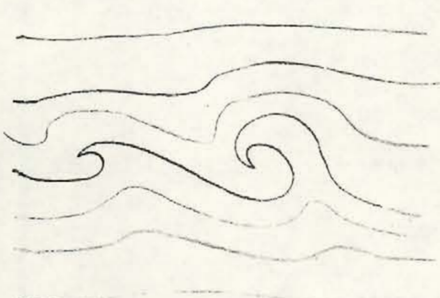

Fig. 4. Eddies in a Surface of Discontinuity.

together represents a steady flow of the mean value.

If the velocity components are denoted by u_m v_m and the temporary deviations from those by u' v' so that the actual velocities are $u = u_m + u'$, $v = v_m + v'$ then the mean values of u' v' are zero. By definition this is however, not true of the mean of the squares of the products of u' and v'.

In applying the momentum theorem to turbulent motions it is not sufficient to apply it to the steady average motions but the mean value must be formed from the momenta crossing the fixed control surface. It can be shown that the average momentum passing through a unit area is

$$\rho(u\ v)_m = \rho u_m v_m + \rho(u'\ v')_m$$

where the suffix "m" is used to denote the mean values. This means that the average momentum passing through this area is greater than that calculated, using the average velocities, by the amount $\rho\ (u'\ v')_m$ the mean value of the product of the velocity fluctuations.

Now the change of momentum with time of any mass is equal to the force acting on that mass. Therefore the reaction corresponding to $\rho\ (u'\ v')_m$ which is exerted on a unit area is a shear stress, and

$$\tau' = -\rho(u'\ v')_m \quad \text{..............................} \quad (4)$$

where τ' is an apparent shearing stress caused by turbulence. This equation cannot be applied because of the difficulty of estimating a value for τ'.

In order to obtain a formula of practical use Prandtl expressed u' and v' the fluctuations of velocity by other quantities related to the distribution of the mean velocity. Prandtl assumed a length which he considered related to the diameter of balls of fluid which move as a whole, and also as the path transversed by those balls relative to the rest of the surrounding fluid.

Considering a ball of fluid displaced between two velocity layers of distance ℓ apart the change in its velocity v' becomes $\ell \frac{du_m}{dy}$. Because of the continuity condition for a small element the velocity fluctuation v' must be of the same magnitude. Inserting these values for u' and v' in equation (4)

$$\tau' = \rho \ell^2 \left(\frac{du_m}{dy}\right)^2 \quad \ldots\ldots\ldots\ldots\ldots\ldots\ldots (5)$$

This is Prandtl's equation and it can be applied to many problems of turbulent flow.

If we assume that $\epsilon = \rho \ell \frac{du_m}{dy}$ then

$$\tau' = \epsilon \frac{du_m}{dy} \quad \ldots\ldots\ldots\ldots\ldots\ldots\ldots\ldots (6)$$

and the equation becomes of the same type as the equation for the viscous shearing stress $\tau = \mu \frac{du}{dy}$ and ε has the dimensions of a viscosity. It is however larger by power of ten. Another important difference is that it varies very much from point to point, for example it goes to zero as the boundary wall is approached.

The mixing length ℓ in turbulent motion varies from place to place. No general theory is yet available regarding its magnitude, although in a number of particular cases it has been found possible to make assumptions leading to results in good agreement with experiment. In many instances it is permissible to neglect the actual shearing stresses arising from the viscosity in comparison with the apparent shearing stresses, and also a far more reaching assumption to leave the effect of viscosity on the magnitude of ℓ out of account altogether. The latter assumption is permissible only for large Reynolds' numbers.

In many cases the length ℓ can be brought into a simple relation to the characteristic lengths of the respective flows. For the flow along a smooth wall ℓ must at the wall itself equal zero, since all transverse motions are prevented at solid boundaries.

In order to find the quantity ℓ from the data of basic flow, T. Kármán put the ?

$$\ell = k \left| \frac{du}{dy} \right| \left| \frac{d^2u}{dy^2} \right|$$

according to the formula ℓ is not dependent on the amount of velocity but only on the velocity distribution. Thus ℓ is a pure position function, k is a constant which must be determined from experiment.

The Prandtl mixing length formula has been applied successfully to cases of free jets issuing in still air. Here the mixing length ℓ may be assumed a pure position function proportional to the width of the jet: from the resulting formula we can deduce their behaviour.

The difficulty of applying Prandtl's equation to calculations for the injector is one of finding a suitable mixing length. With an injector having a large ratio of mixing tube diameter to primary nozzle diameter it is probable that in the region of the exit of the primary nozzle the mixing length ℓ would be closely related to the mixing length of the free jet. Of course, as the mixing advanced, this simple assumption could not apply, since near the wall the mixing length must become zero. It is therefore unlikely that any simple approximation for the mixing length would yield valuable results without investigating the velocity, pressure and turbulence in the mixing tube.

III Review of Literature

In the published work on injectors most authors consider only the one-dimensional analysis of entrance to and exit from the mixing tube. Mixing is considered to take place either at constant area or constant pressure, the two cases subject to calculation. This type of analysis is exemplified by work of Stodola (Ref. 14) and later by Flügel (Ref. 4).

In his analysis of the injector Flügel considered mixing to take place at constant pressure. By using the energy equation he arrived at optimum velocities for mixing of the primary and secondary fluids. Combining the energy and momentum equations he was able to outline calculations for an injector with constant pressure mixing followed by a diffuser. From his calculations he was able to suggest the best shape of mixing nozzle and he presented equations which applied to gas liquids and vapours.

Flügel introduced the concept of the effective dragging force between primary and secondary fluids. To simplify the calculations he assumed that at any point the velocity over a section of the primary jet and the velocity over the annular area occupied by the secondary fluid were constant. He applied the following formula

$$df = k \frac{\rho}{2g} (v_1 - v_2)^2 \; da$$

where "df" is the force on a small element "da" of the boundary surface, "k" a kind of friction constant and "v_1" and "v_2" the velocities of the fluid streams. By applying this equation together with the momentum equation for small sections of length "dx" along the axis, and allowing for wall friction, he obtained an equation which may be solved for liquids but is insoluble for dissimilar compressible fluids.

A similar approach has more recently been made by B. Szczeniowski (Ref. 16). By equating the resistance of the primary on the secondary fluid he was able to calculate the performance of a liquid injector. His calculations are concerned only with end results and unlike Flügel's do not follow changes along the mixing tube.

Keenan and Newmann (Ref. 8) studied an air injector with constant area mixing. By varying the diameter of the primary nozzle they investigated a range of diameter ratios of primary nozzle to mixing tube from 107 to 1024. The apparatus was designed with a blower for the secondary air so that tests could be run with equal pressures before the secondary nozzle and at the exit of the mixing tube. Most of the experimental results are given for this condition and therefore cannot be used for pump design. They found that in the region of variables investigated their results agreed fairly closely to that predicted by one-dimensional treatment.

CHAPTER III

APPARATUS

The apparatus was designed to study the pumping properties of the injector and the pressure behaviour in the mixing tube. It was thought that the most useful information could be obtained by keeping the geometry of the injector as simple as possible, so an injector with a constant mixing tube diameter was chosen. This type of injector gives a pressure rise in the mixing tube and lends itself to one-dimensional analysis.

In choosing the range of variables for the injector the possibility of using the same injector later as a coal pump was kept in mind so that comparisons could be easily made. A range of diameter ratios of primary nozzle to mixing tube of between 2.24 to 5.73 was chosen with pressure ratios across the primary nozzle from 2 to 6.

A layout of the apparatus is shown in Fig. 5. The air for the primary nozzle was supplied from the laboratory main and was capable of giving 0.1 lbs per second at 90 psia. The air flowed through a globe valve with a bypass for fine adjustments and through a standard orifice meter before passing to the primary nozzle. The pressure and temperature of the air before the orifice meter was measured and also the differential pressure across the orifice plate.

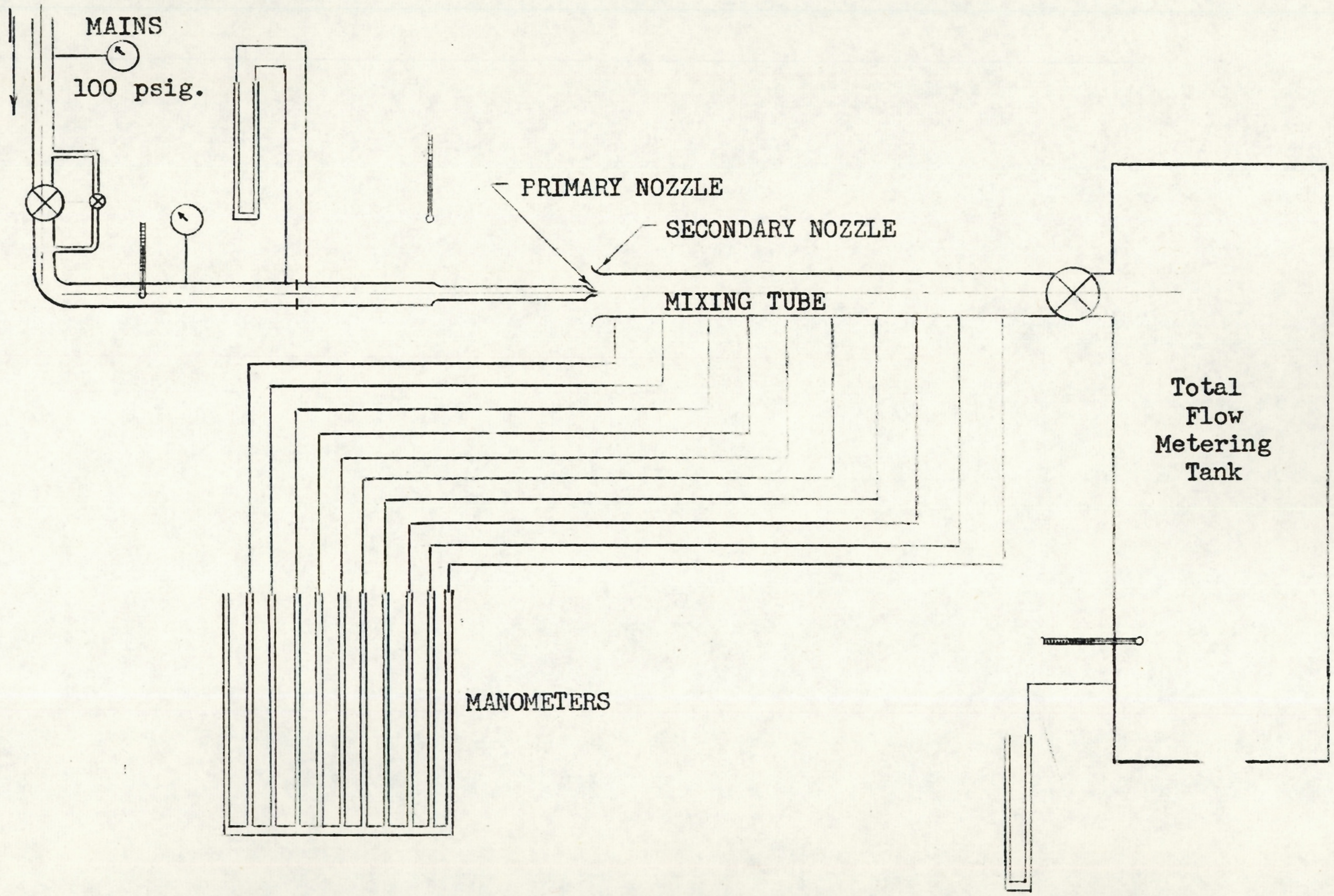

Fig.5. Layout of Apparatus

Fig.6. Detail of Primary Nozzle

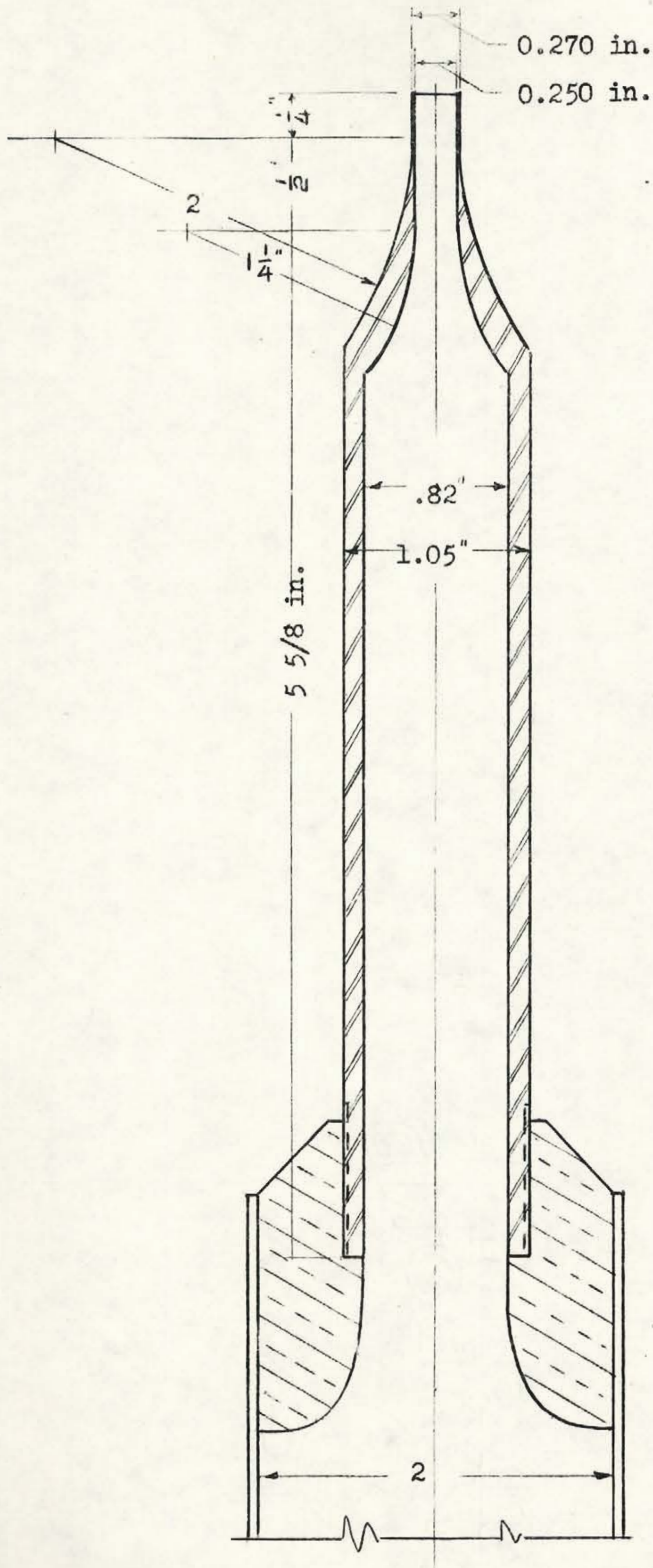

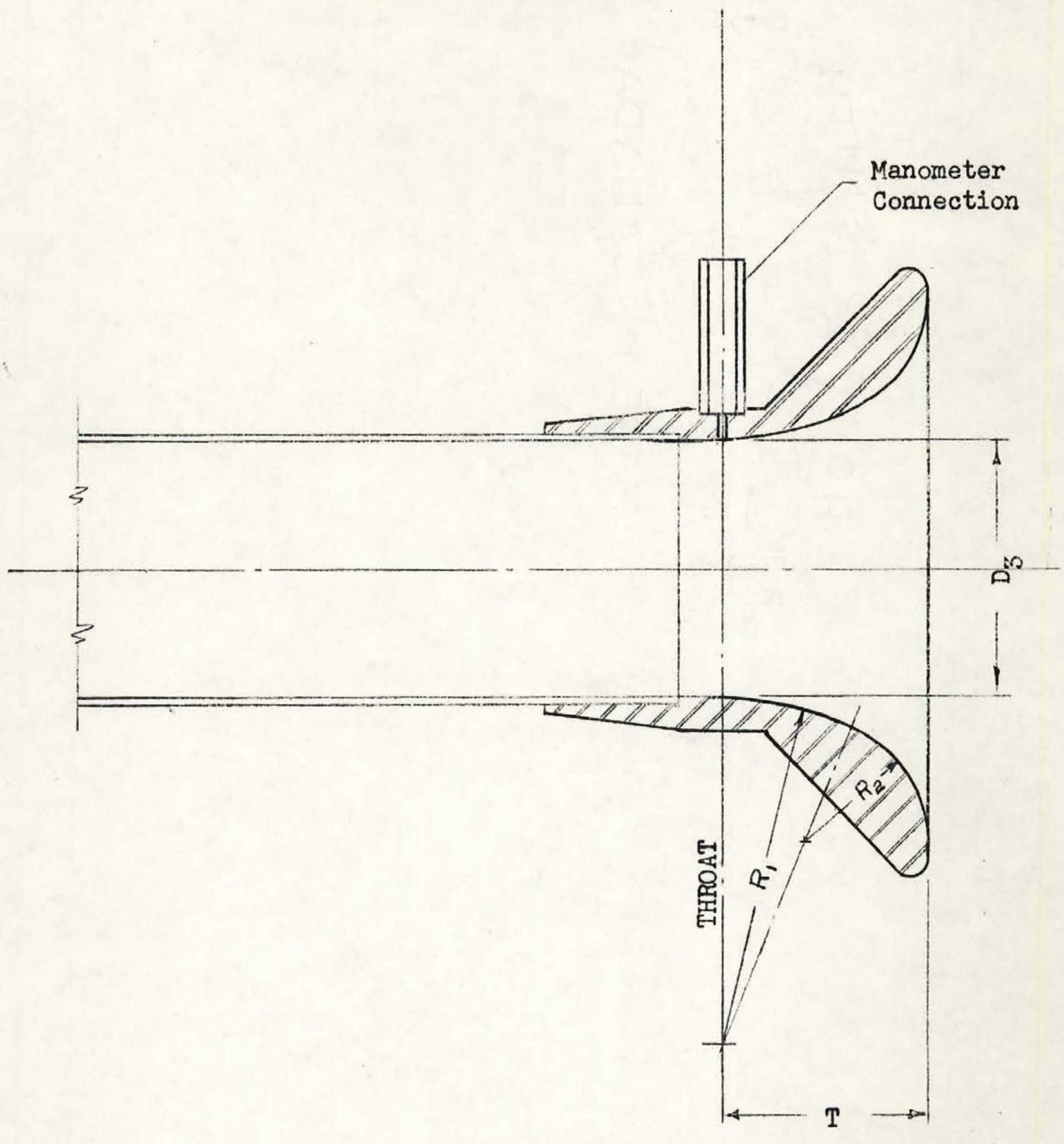

Fig.7. Details of Secondary Nozzle

Nozzle No.	D_3 in.	R_1 in.	R_2 in.	T in.
1	1.433	1.92	0.68	1.156
2	1.187	1.56	0.56	0.937
3	0.811	1.12	0.40	0.656
4	0.560	0.80	0.28	0.469

The details of the primary nozzle are shown in Fig. 6. The outside profile of this nozzle was designed so that the secondary flow into the mixing tube would not be restricted when the primary nozzle was located at the throat of the secondary nozzle. The inside of the primary nozzle was shaped to reduce losses.

The secondary nozzles were machined from brass with profiles and diameters shown in Fig. 7. In order to obtain these profiles very accurate templates were first made and then the nozzles machined to match them. The profiles are close to the A.S.M.E. Bell-mouth orifices (Ref. 2).

The throat of the nozzles were of the same inside diameter as the mixing tubes. These tubes were made from stainless steel tubing of 5/8", 7/8", 1-1/4" and 1-1/2" nominal diameter and about 32" long. They were threaded at the ends to facilitate changing.

A series of pressure taps were made to determine the static pressure rise along the mixing tubes. This was a convenient way of determining the lengths required for fluid mixing, and offered many advantages over methods of other investigators (Ref. 8) who made the mixing tube sectional and increased or decreased the length by attaching or removing sections.

Pressure taps were provided at the throat section of the secondary nozzles as shown in Fig. 7 and also every two inches along the tube. A convenient way of attaching the

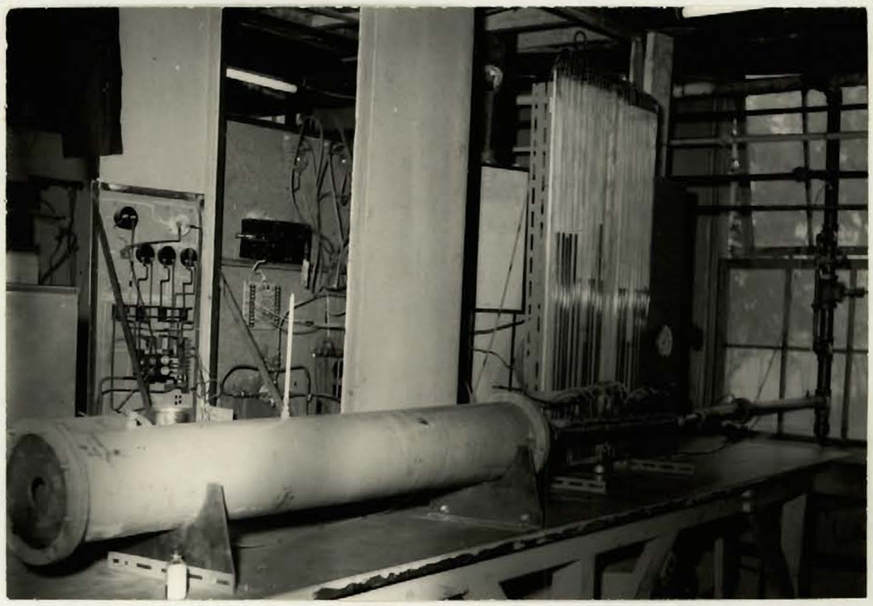

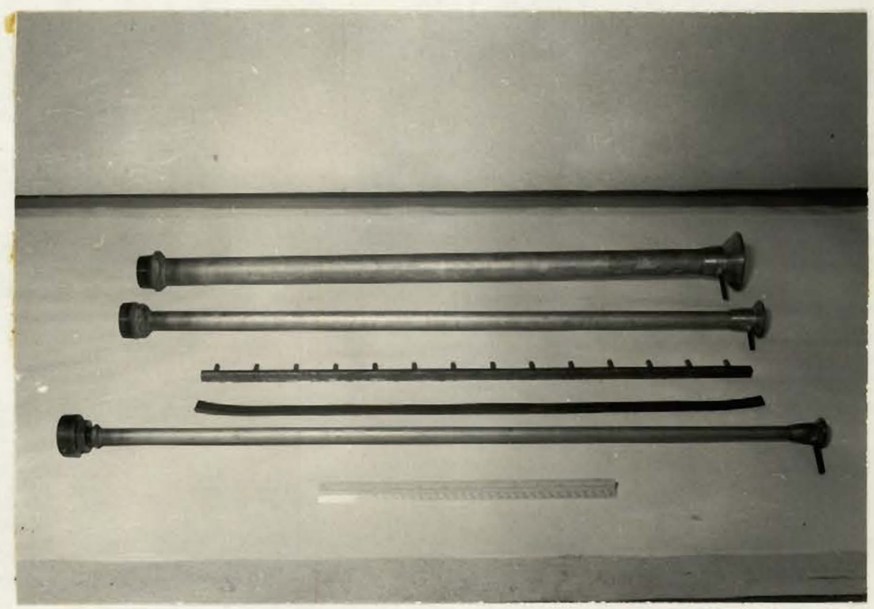

Fig.8. Photographs of Rig Showing Manometer Tube Attachment

manometer lines was used, see Fig. 8. The tube was drilled and a metal strap with the manometer connections was clamped to the mixing tube and provided with a rubber gasket to prevent leaks. This arrangement eliminated any possibility of tube distortions caused by welding on the manometer connections. It also made the initial construction easier and saved considerable time when the tubes were changed.

An air metering tank was placed after the injector with a valve to control the pressure rise in the mixing tube. The tank itself was about 6 feet long and 8 inches in diameter provided with a baffle at the inlet to even out the velocity. A 1.999 in. diameter thin plate orifice was provided at the outlet end to measure the total flow through the injector. Provision was made to measure the temperature and pressure of the tank.

CHAPTER IV

EXPERIMENTAL PROCEDURE

I Calibration of Meters

Before proceeding with the injector tests the instruments were checked and the meters calibrated. The thermometers were compared with a primary standard thermometer at room temperature and agreed within 0.3°F. The primary air gauge was compared with a Gas Dynamics Laboratory's standard pressure gauge and found to agree within 0.1 psi. throughout its entire range.

The apparatus contained three flow meters. The first was a standard thin plate orifice meter with flange taps. The mass flow formula and coefficient for this meter was taken from reference 2. The second fluid meter was the primary nozzle itself. The third meter was the total flow meter and for this a coefficient given by Gamberg was used (Ref. 2).

The first test was made to calibrate the primary orifice plate meter against the primary nozzle. Readings were taken with the pressure upstream of the orifice plate adjusted to 30, 50, 70 and 90 psia. From this run the formula given for the primary air flow in Appendix I was calculated.

The second test was made to check the primary orifice plate meter against the total flow meter. For this test the primary nozzle and the mixing section were removed and the primary thin plate orifice meter connected in series with the total flow meter. The test was run at approximately the same conditions for the primary orifice plate meter as in the first calibration run. The mass flows calculated for both meters agreed within 1%.

INSTRUMENT LIST

		INSTRUMENT	RANGE	SMALLEST SUBDIVISION
PRESSURES	1. Laboratory mains air pressure at inlet to apparatus	Pressure Gauge	0 - 100 psig.	0.5 psi.
	2. Air upstream of thin plate primary orifice	Pressure Gauge	0 - 100 psig.	0.5 psi.
	3. Differential pressure across primary orifice	H_2O Manometer	0 - 40" H_2O	0.1"
	4. Atmospheric Pressure	Hg. Barometer		0.01"
	5. Mixing tube static pressures	H_2O Manometers	0 - 40" H_2O	0.1"
	6. Total flow metering tank pressure	H_2O U-tube	0 - 40" H_2O	0.1"
TEMPERATURES	7. Air temperature upstream of primary orifice	Mercury Thermometer	0 - 120°F	1°
	8. Ambient Air Temperature	Mercury Thermometer	0 - 120°F	1°
	9. Total flow measuring tank temperature	Mercury Thermometer	0 - 120°F	1°

II Experimental Running

Throughout the injector tests the primary and secondary air remained close to room temperature and the secondary air was at all times the prevailing barometric pressure. The primary nozzle was located on the same axis as the mixing tube, this left the following five variables.

(1) Distance from the exit of the primary jet to the throat of the secondary nozzle. In the apparatus this could be adjusted to any desired value.

(2) The diameter ratios of mixing tube to primary nozzle. Ratios of 2.24, 3.24, 4.75 and 5.73 were obtainable.

(3) The pressure ratio across the primary nozzle. Any value up to 6 could be obtained.

(4) The pressure rise ratio across mixing tube. This could be varied but its maximum value depended on the other variables.

(5) The secondary air mass flow, its value also was governed by the other variables.

A test was performed to determine the effect of varying the distance from the exit of the primary jet to the throat of the secondary nozzle. During this test the mixing tube diameter and the primary air pressures were kept constant at values of 1.187 and 40 psia. respectively. One test was carried out at a constant low pressure in the mixing tube of 0.329" Hg. and varying the location of the primary nozzle from 0.7 mixing tube diameters inside the throat to 4.75 diameters outside the throat. In this test the secondary mass flow became the dependent variable.

A second test similar to the previous one was carried out but this time the pressure rise in the mixing tube was adjusted to a higher value; the secondary flow was very small so it was kept constant and the pressures in the mixing tube allowed to vary. This concluded these tests.

A comprehensive series of tests were then performed to determine the effect of varying (2), (3) and (4) on the performance of the injector. For these tests the exit of the primary nozzle was located at the throat of the secondary nozzle. The procedure for these experiments all followed a similar pattern. With one of the mixing tubes in place the primary air pressure was kept constant at 30 psia. and a series of readings taken varying the pressure in the mixing tube. Then the pressure was increased to 50, 70 and 90 psia. and a set of readings obtained for each of those pressures. The mixing tube was then replaced with one of a different size and the same procedure followed. In this way the full range of variables was covered.

The results of these tests are shown in Figs. 22 to 33 inclusive. The static pressure behaviour along the walls of the mixing tube are presented as curves and the values of the variables that were kept constant for each particular curve are shown.

CHAPTER V

DISCUSSION OF RESULTS

I - Effect of Position of the Primary Nozzle

The results of changing the axial position of the primary nozzle relative to the mixing tube are shown in Figs. 10 and 11. For both curves the primary pressure was kept at 40 psia. and the mixing tube diameter at 1.187 inches. For Fig. 10 the pressure in the mixing tube p_3, was kept constant at the low value of 0.353" Hg. The graph shows that from a distance of about one mixing tube diameter outside the throat of the secondary nozzle to about 0.5 diameters inside the throat, the ratio of M_2/M_1 remains constant at its maximum value. From one diameter to 4.75 diameters outside the throat the ratio M_2/M_1 decreases almost linearly with distance; also if the nozzle is advanced more than 0.5 diameters inside the throat of the secondary nozzle the ratio M_2/M_1 decreases, because of the shape of the primary nozzle which restricts the secondary flow. The best position of the primary nozzle is close to the throat of the secondary nozzle when the values of p_3 are small. Similar results have been found by Keenan and Neumann (Ref. 8) when investigating larger diameter ratios with low mixing tube pressures.

The effect of varying the position of the primary nozzle was also investigated with the pressure in the mixing tube increased to approximately 3.05" Hg. (Fig. 11). Because the secondary flow was very small it was kept constant and p_3 allowed to vary. The best position for the primary nozzle was, in this case, between three and four mixing tube diameters outside the throat of the secondary nozzle. It would seem that the best position of the primary nozzle depends on the pressure rise ratio in the mixing tube. However when the primary nozzle is located at the throat of the secondary nozzle the decrease in pressure rise from the maximum value is only 0.25" Hg.

It is interesting to note the effect of the position of the primary jet on the static pressure behaviour in the mixing tube. Figs. 10 and 11 show that varying the position of the primary nozzle changes the position of the static pressure curve but the curves remain similar for all primary nozzle positions.

II Behaviour of the Static Pressure in the Mixing Tube

Figs. 30, 31, 32 and 33 show the behaviour of the static pressure along the wall of the 1.433 in. diameter mixing tube. These curves show that, in general, for a short distance after the throat of the secondary nozzle the static pressure increases linearly with distance. Then there is a region where the pressure increases very rapidly: finally the static pressure becomes fairly constant with a slight decrease which is due to frictional losses. As shown, the behaviour of the pressure at the section of the mixing tube close to the secondary nozzle depends on the M_2/M_1 ratio. For high values of this ratio the static pressure increases, but for the very low values of M_2/M_1 the pressure decreases slightly.

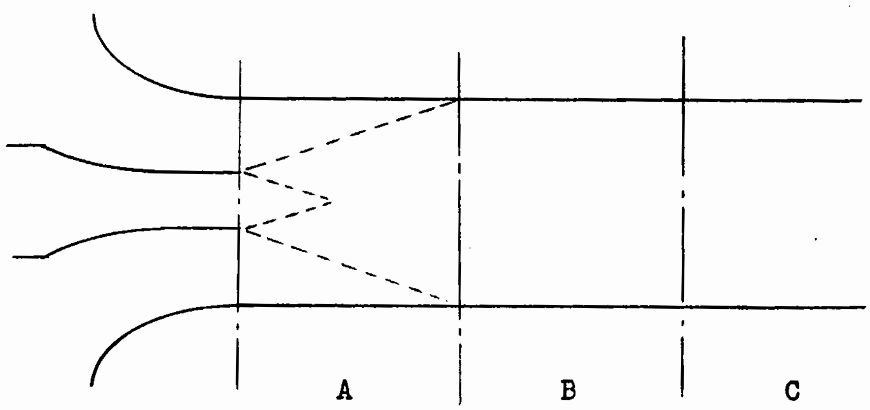

Fig. 9. Regions of Mixing Tube.

The first part of the pressure curves correspond to region "A" of the diagram (Fig. 9). The position of maximum slope corresponds to region "B" where the boundary of the jet reaches the wall. The constant pressure part of the curves corresponds to region "C" where the mixing is complete.

With the curves for the smaller diameter mixing tubes the first constant slope sections of the static pressure curves are not as definite. This is probably due to region "A" being shorter and so the widely spaced pressure taps could not detect it.

III Mixing Length

An attempt was made to determine the factors affecting the length required for mixing the fluid streams. Mixing length* may be defined as the distance from the exit of the primary nozzle to the point where the pressure rise in the mixing tube reaches its maximum value. However it is difficult to locate the maximum pressure rise from the pressure profile curves but points where the pressure rise is 95% of the maximum can be located more easily. These points were therefore used to correlate the mixing length to the other variables.

The ratios of the mixing lengths to the tube diameters were calculated and plotted against mass flow ratios M_2/M_1 as shown in Figs. 12, 13 and 14. From these curves it can be observed that L/D_3 increases as M_2/M_1 increases, this relation being linear in the case of the 0.560 in. and the 0.811 in. diameter mixing tubes.

If the curves are extended, then for the case where no secondary fluid is flowing the mixing length is approximately 4.5 mixing tube diameters in all cases. When M_2 is equal to M_1 then the L/D_3 ratio increases as the M_1 increases. The length required for mixing varies from about 4.5 mixing tube diameters to 10.5 diameters.

---

* The mixing length as defined above is not to be confused with Prandtl's mixing length, as mentioned in Chapter II.

IV General Performance of Injectors

In Fig. 15 lines are drawn for constant diameter ratio showing the relation between M_2/M_1 and p_3/p_o and pressure constant at 30 psia. The curves all behave similarly in that the values of M_2/M_1 decrease as p_3/p_o increases, this relation being almost linear. The relationship of M_2/M_1 depends on the diameter ratio.

The lines for larger diameter ratios are more closely parallel with the M_2/M_1 axis and the smaller diameter ratios more closely parallel to the p_3/p_o axis. Lines predicted from theory are also shown in this graph. These lines show a marked similarity with the experimental curves.

When the envelope is drawn to the constant area curves the resulting curve will show the maximum value of M_2/M_1 for any given value of p_3/p_o. It also shows that for any value of p_3/p_o there will be a best diameter ratio that will give the maximum value of M_2/M_1. This is very important in the design of injectors.

Similar curves for constant primary pressures of 50, 70 and 90 psia. are shown in Figs. 16, 17 and 18. They all behave similarly to the 30 psia. curves. Also, the curves predicted from theory show a very marked resemblance to the experimental curves.

In order to compare the curves for different pressures a set of envelope curves are drawn from the experimental curves of 30, 50, 70 and 90 psia. primary pressures. It will be seen that the effect of increasing the primary pressure is to shift the envelope curve away from the M_2/M_1 and p_3/p_o axes. For a given value of p_3/p_o the value of M_2/M_1 will increase as the primary pressure is increased, provided of course the optimum diameter ratio is used in each case.

It will be noted that the theoretical curves agree more closely with experimental curves of higher primary pressures. By trial and error it was found that if theoretical curves are drawn for 70% of the actual pressure ratio then these envelope curves agree fairly closely with experimental curves (Fig. 20). This offers an approximate method of predicting the performance of the injector from one-dimensional curves.

Points were located in Figs. 15, 16, 17 and 18 where the experimental curves touched their envelope curve. From these points a set of design curves were drawn and are shown in Fig. 21. If the required pressure rise in the mixing tube is known and also the pressure that is available for the primary nozzle then the optimum diameter ratio D_3/D_1 can be read directly from this curve.

CHAPTER VI

CONCLUSIONS

Part I

1. In the range of variables investigated the performance of the constant area injector can be predicted closely from one-dimensional theory.
2. The secondary mass flow in the injector decreases as the pressure rise in the mixing tube is increased. This is almost a linear function.
3. For any given value of pressure rise in the mixing tube and pressure ratio across the primary nozzle there is a best diameter ratio D_3/D_1 which will give maximum M_2/M_1. This best diameter ratio can be obtained from curves such as those given in this thesis.
4. No general conclusion can be made regarding the effect of the primary nozzle position on the performance of injectors. However in the cases covered the effect of the primary nozzle position was not critical and good performance was obtained with the primary nozzle located at the throat of the secondary nozzle.
5. The length of tube required for mixing varies from 4.5 to 10.5 mixing tube diameters, increasing as the ratio of M_2/M_1 increases.

Part II

As previously stated the present work on the constant area air injector originated as the preliminary investigation of an injector for pumping solid particles. The results of such an investigation may lead to the design of a simple pump for feeding finely ground solid material against low pressures. A pump of this type could be used for many applications, such as feeding crushed coal to industrial and other types of furnaces. This investigation would be essentially the study of an injector varying the properties of the secondary fluid.

In the limited investigation which was performed on the air injector, the author became aware of the complexity of the injector problem. In the injector not only is the geometry variable but also the fluid properties. To obtain experimental data for the whole range of variables would seem an almost impossible task. In this respect simple methods of analysis such as the one-dimensional treatment is valuable.

There is a great need for fundamental work to be done on the problem of fluid mixing in confined spaces. In the injector the investigation of the region of the primary jet with hot-wire or other instruments should yield valuable information. This would not only clarify the injector problem but also many other related problems.

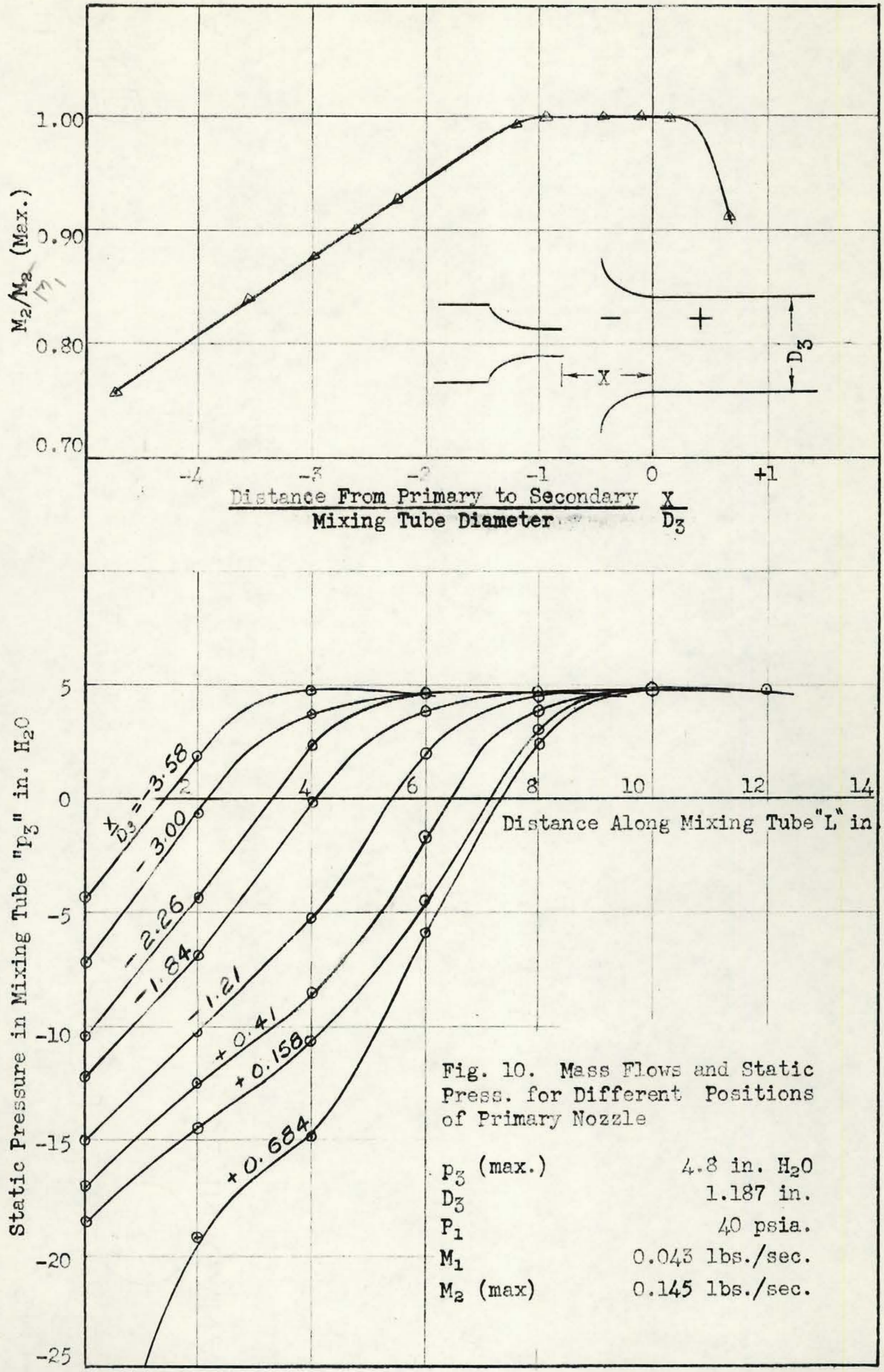

Fig. 10. Mass Flows and Static Press. for Different Positions of Primary Nozzle

p_3 (max.)	4.8 in. H_2O
D_3	1.187 in.
P_1	40 psia.
M_1	0.043 lbs./sec.
M_2 (max)	0.145 lbs./sec.

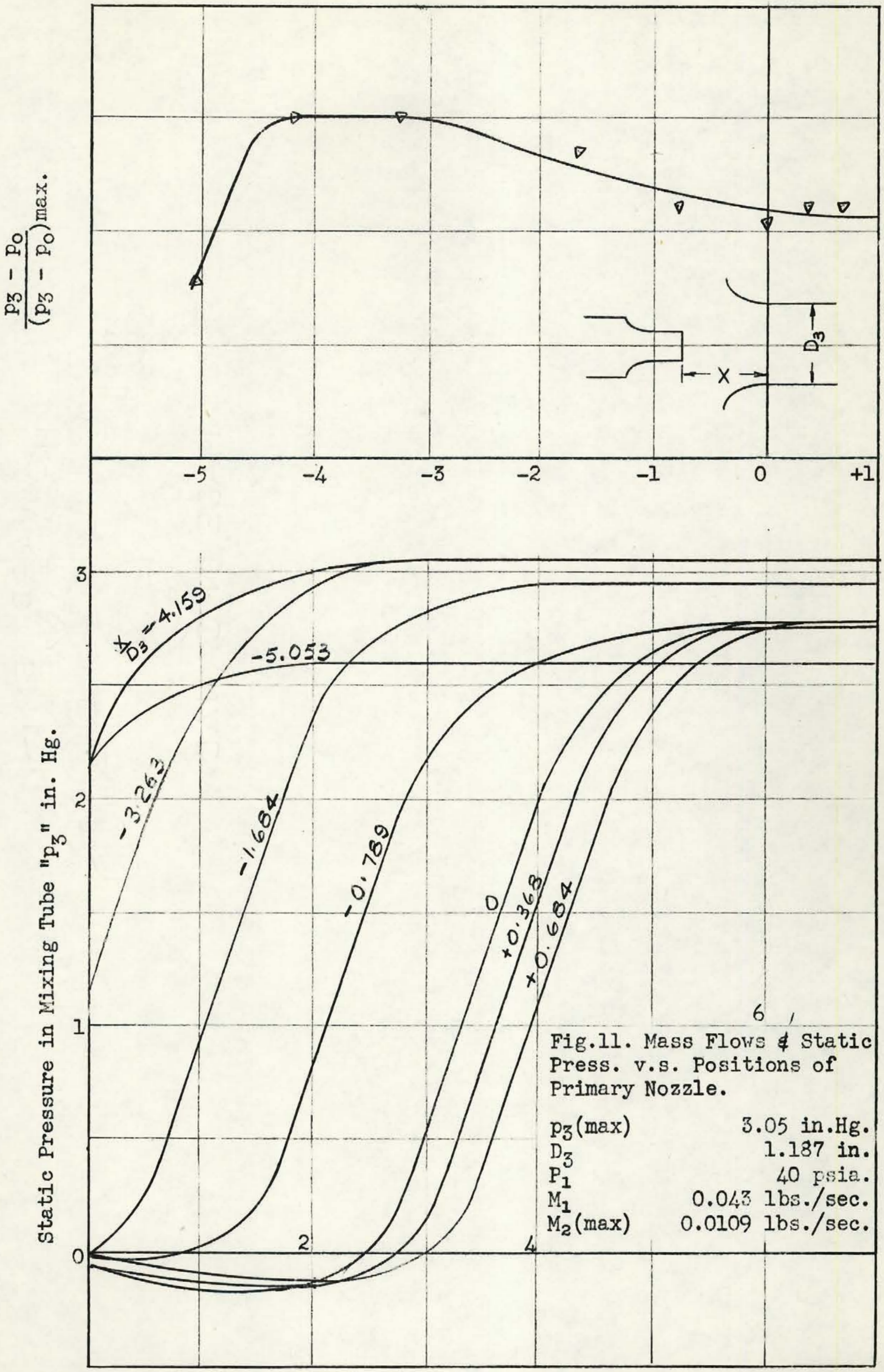

Fig.11. Mass Flows & Static Press. v.s. Positions of Primary Nozzle.

p_3(max)	3.05 in.Hg.
D_3	1.187 in.
P_1	40 psia.
M_1	0.043 lbs./sec.
M_2(max)	0.0109 lbs./sec.

Fig.12. Mixing Length for Diameter

D_3 = 0.560 in.

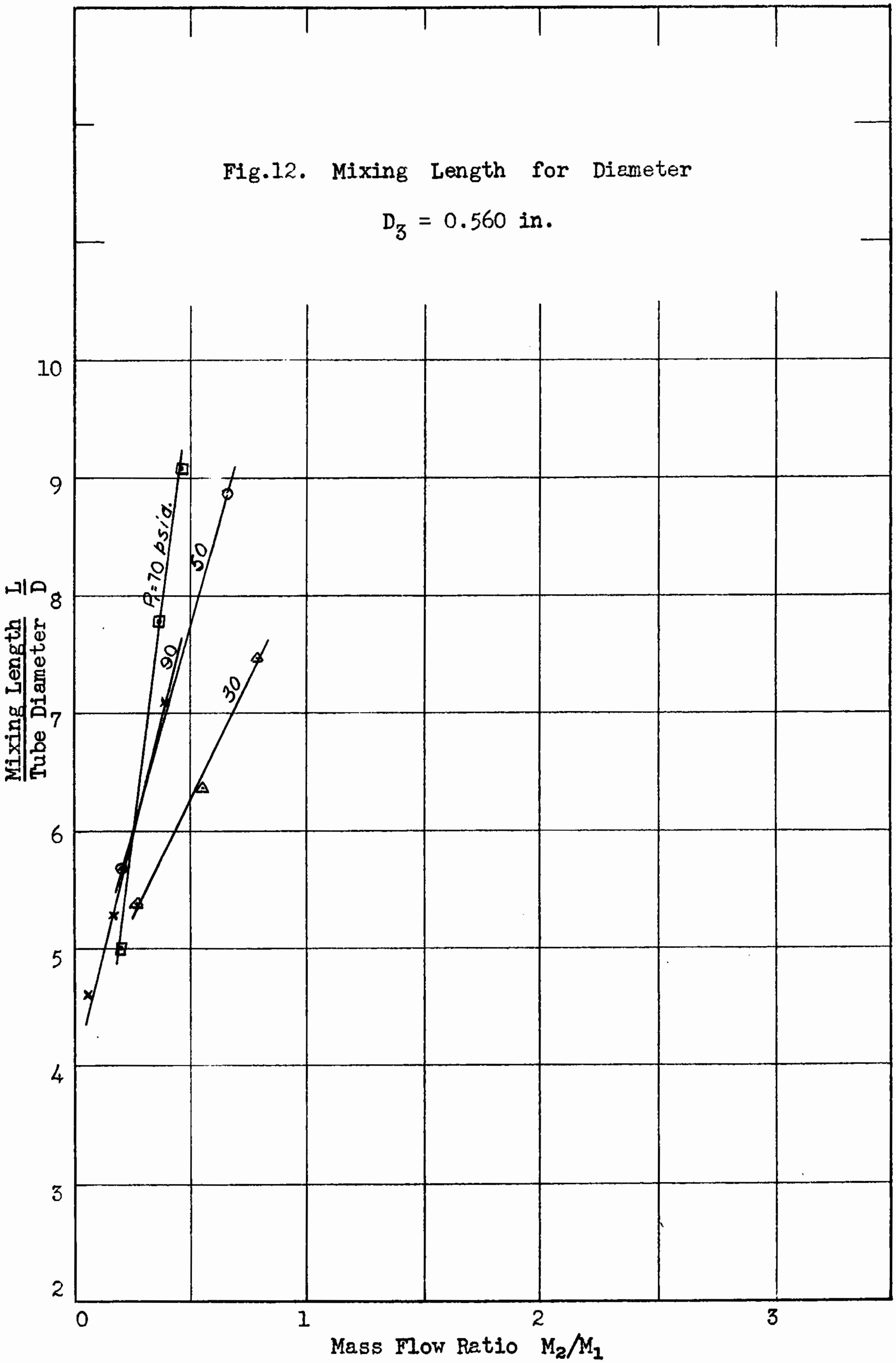

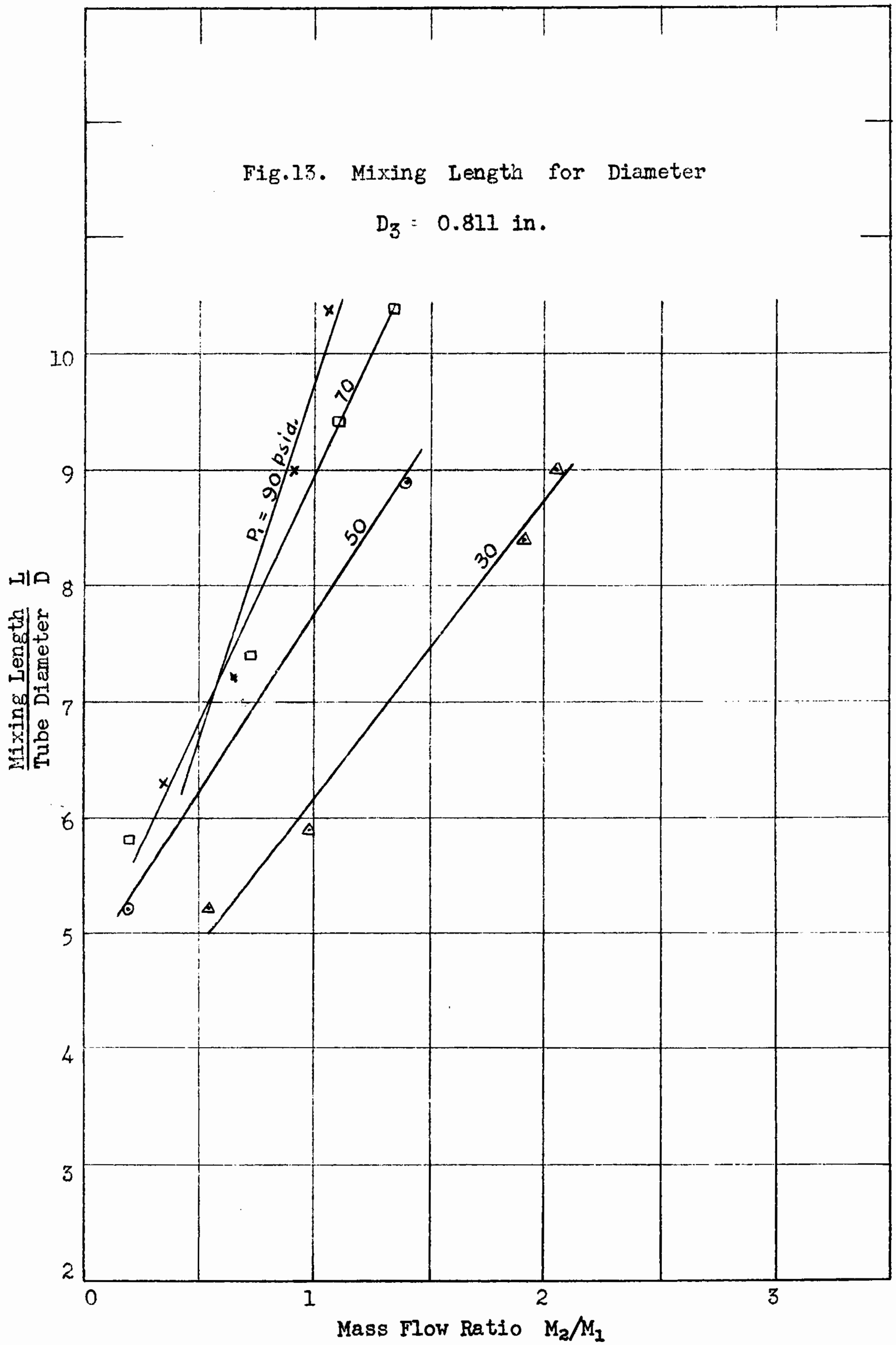
Fig.13. Mixing Length for Diameter
D_3 = 0.811 in.
P_1 = 90 psia.
70
50
30
10
9
8
7
6
5
4
3
2
Mixing Length / Tube Diameter $\frac{L}{D}$
0
1
2
3
Mass Flow Ratio M_2/M_1

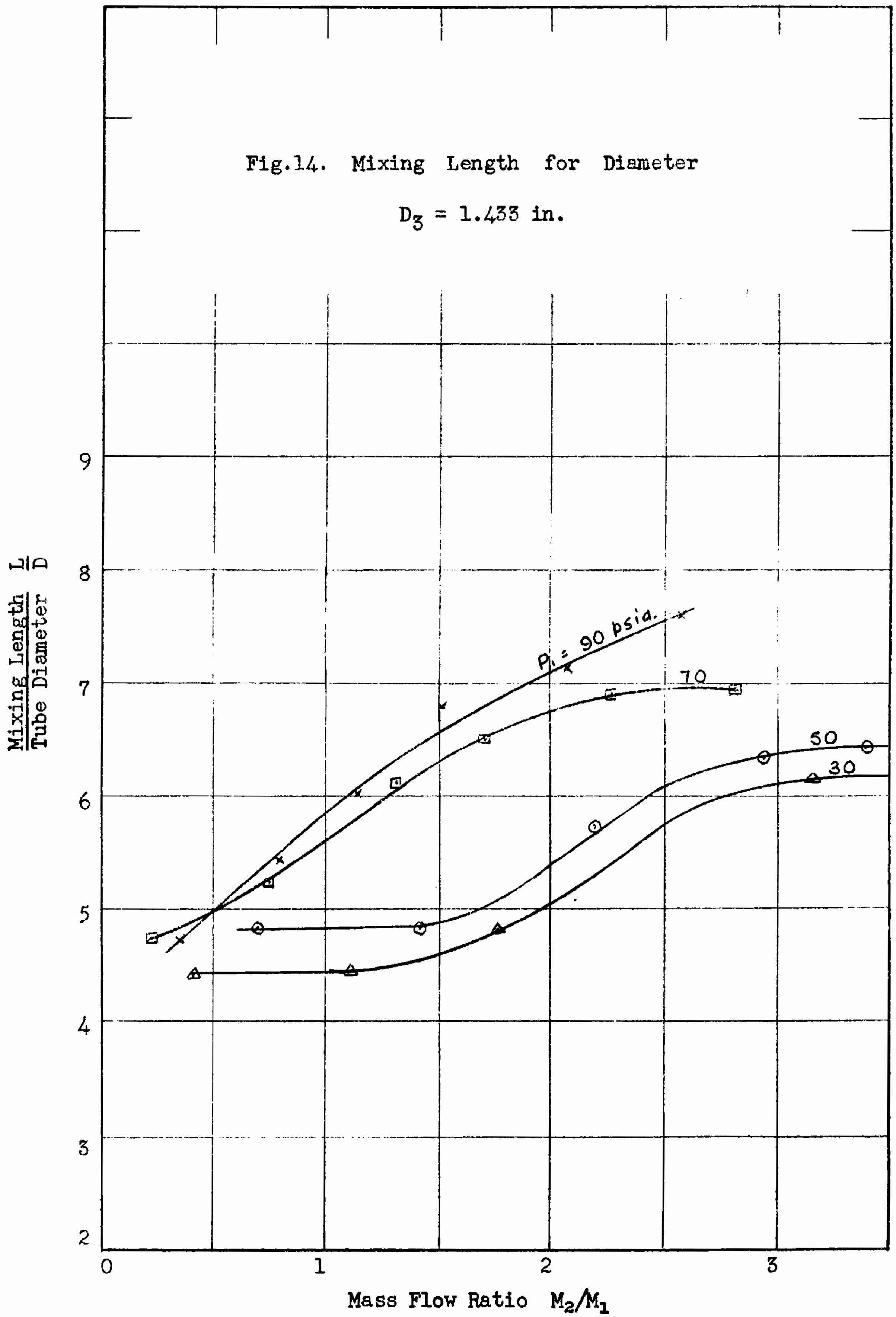

Fig.14. Mixing Length for Diameter

D_3 = 1.433 in.

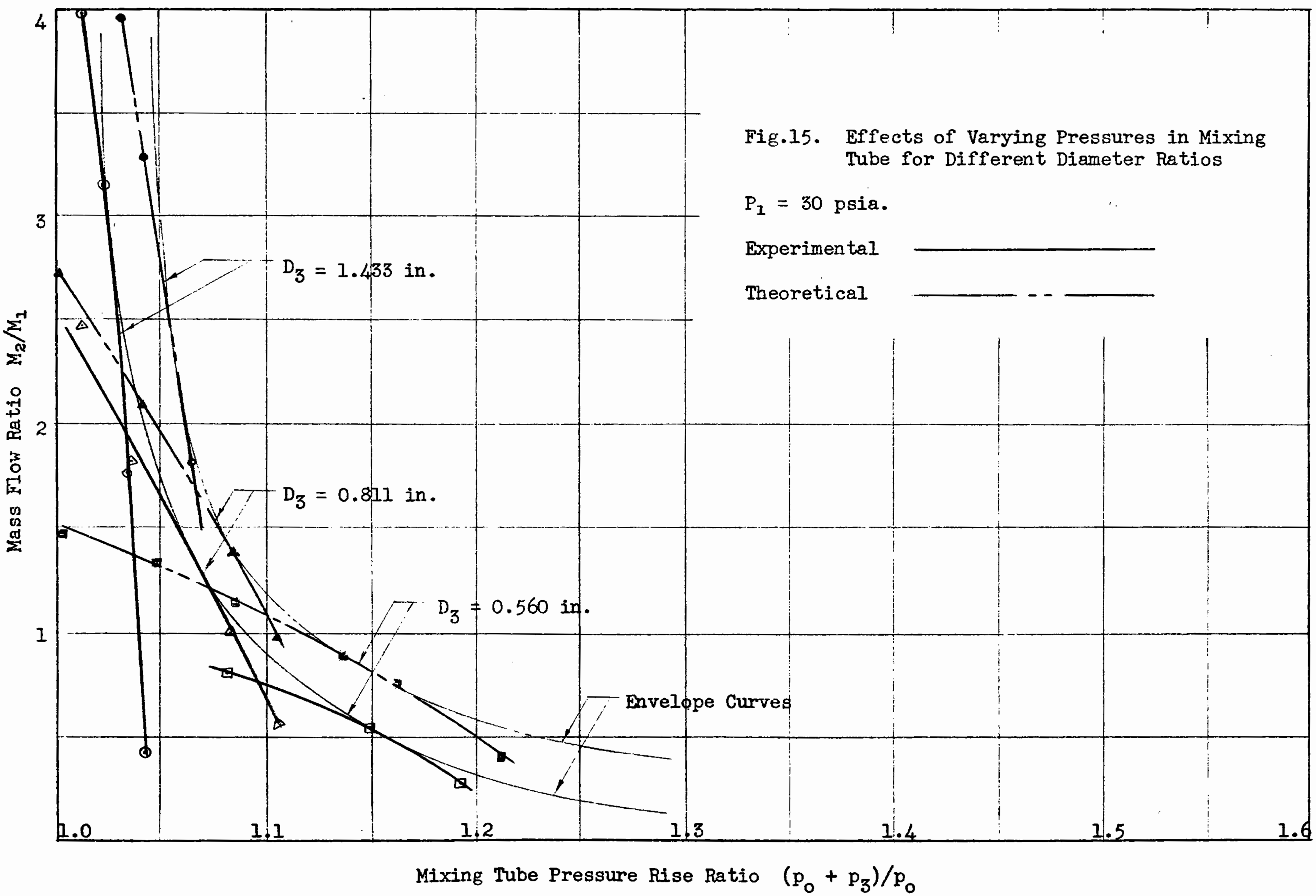

Fig.15. Effects of Varying Pressures in Mixing Tube for Different Diameter Ratios

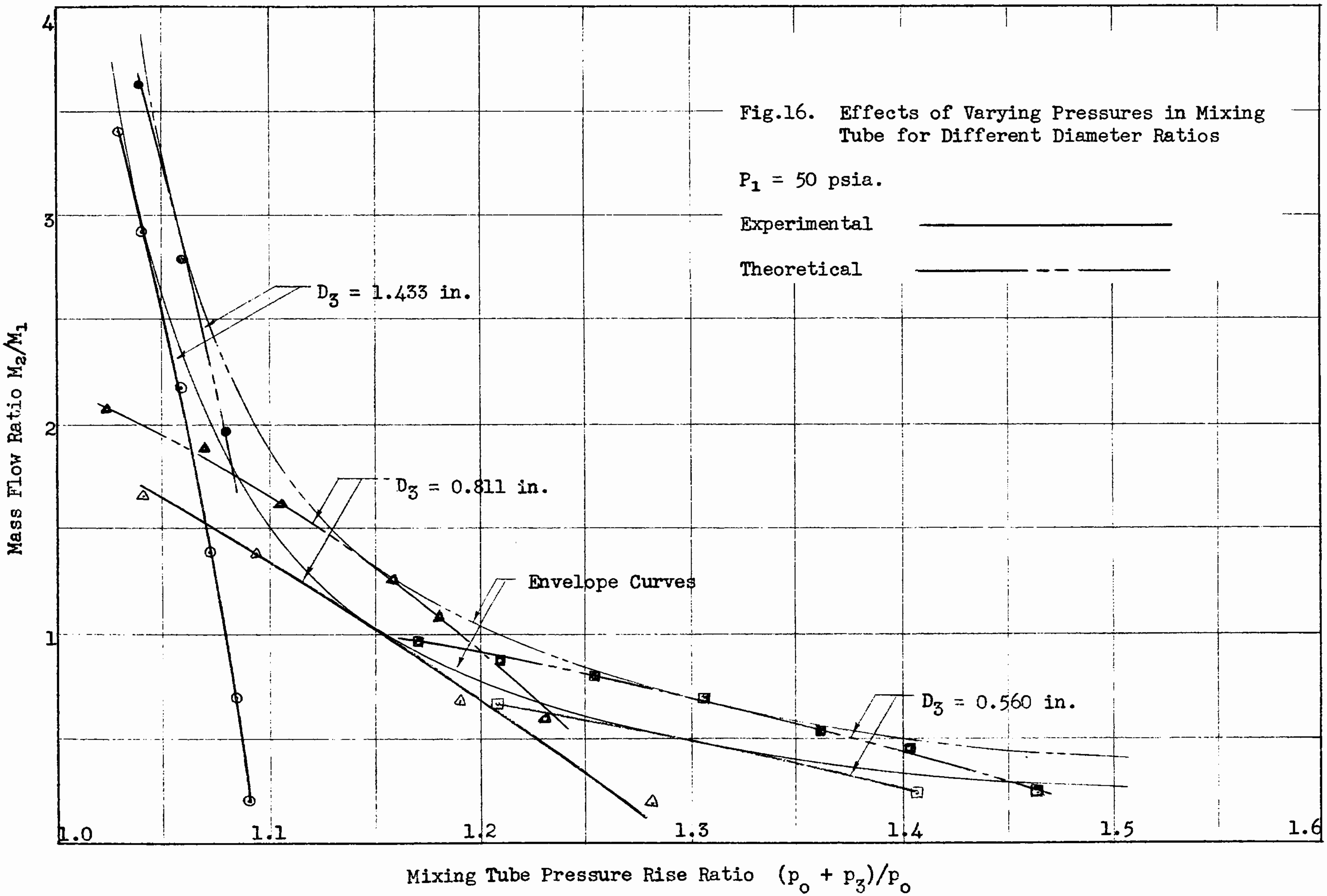

Fig.16. Effects of Varying Pressures in Mixing Tube for Different Diameter Ratios

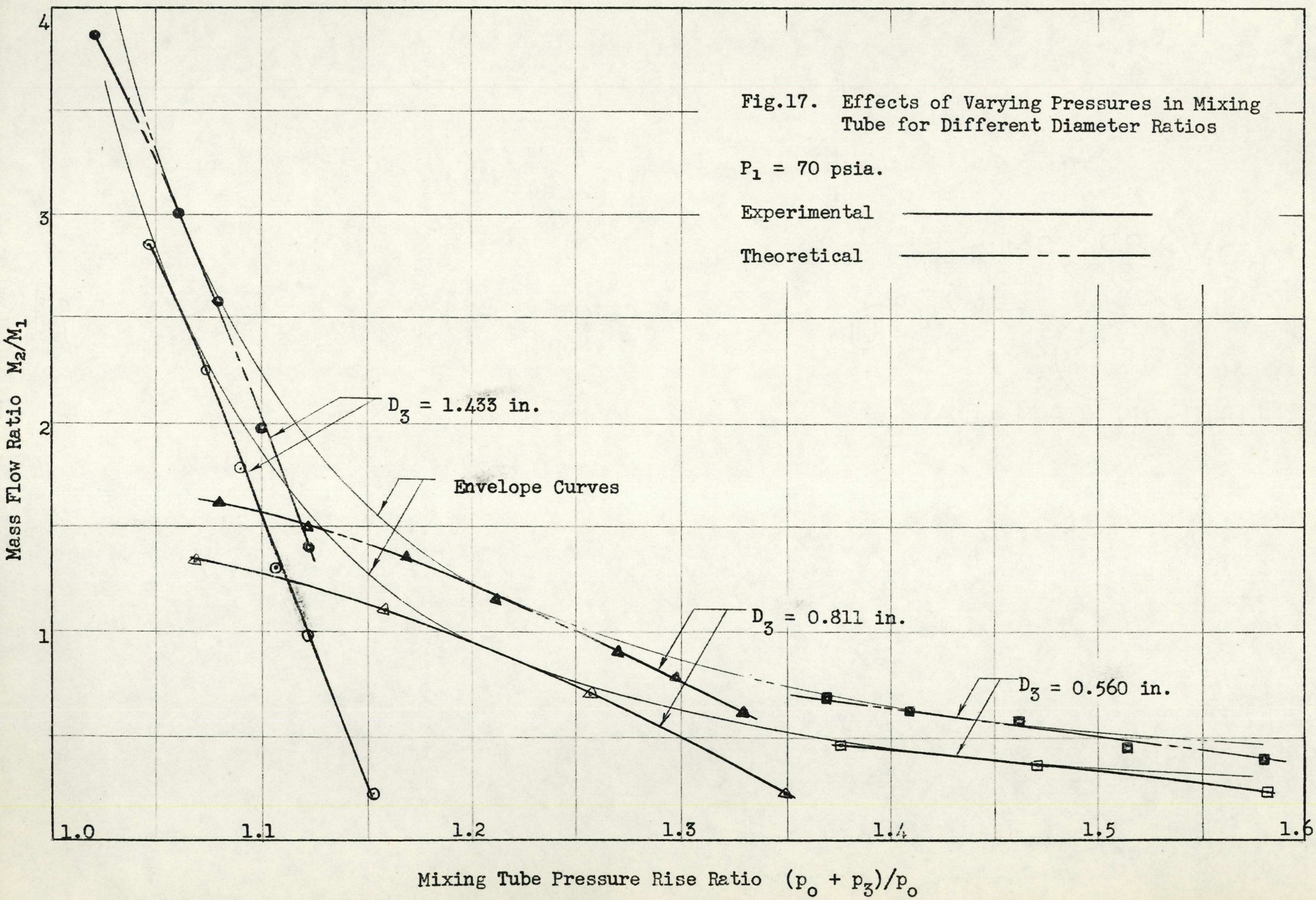

Fig.17. Effects of Varying Pressures in Mixing Tube for Different Diameter Ratios

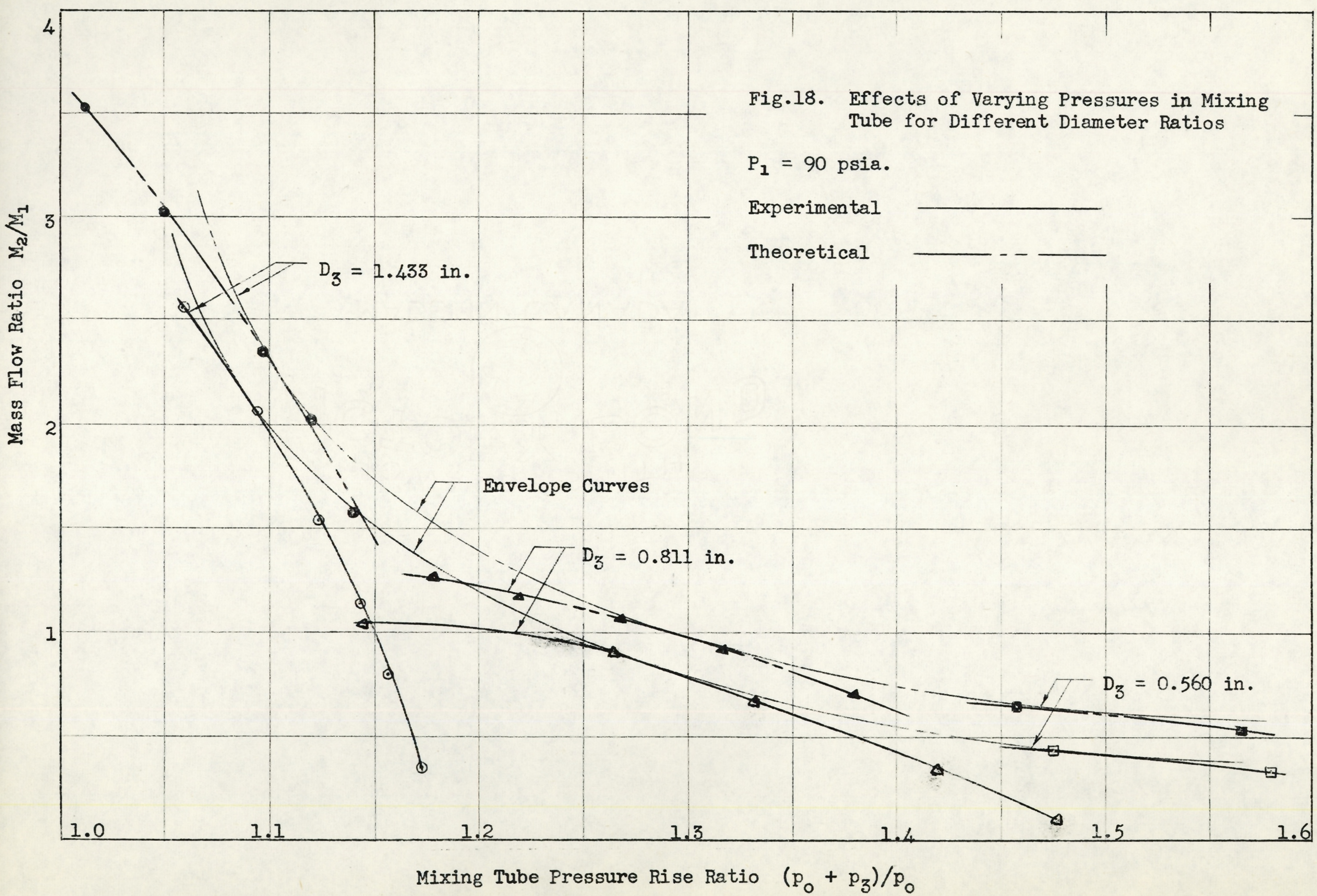
Fig.18. Effects of Varying Pressures in Mixing Tube for Different Diameter Ratios
P_1 = 90 psia.
Experimental
Theoretical
D_3 = 1.433 in.
Envelope Curves
D_3 = 0.811 in.
D_3 = 0.560 in.
Mass Flow Ratio M_2/M_1
Mixing Tube Pressure Rise Ratio $(p_o + p_3)/p_o$
1.0
1.1
1.2
1.3
1.4
1.5
1.6
1
2
3
4

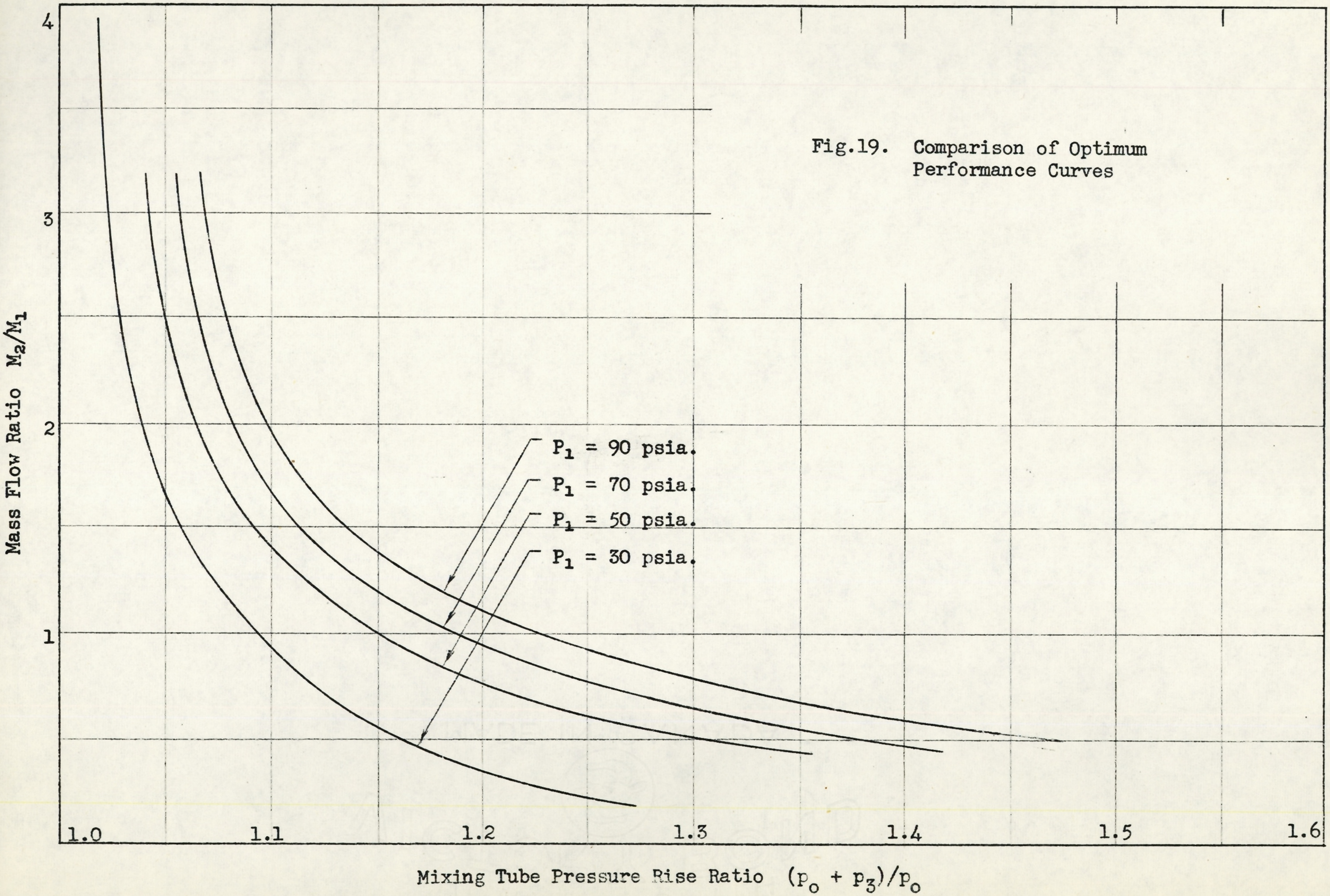

Fig.19. Comparison of Optimum Performance Curves

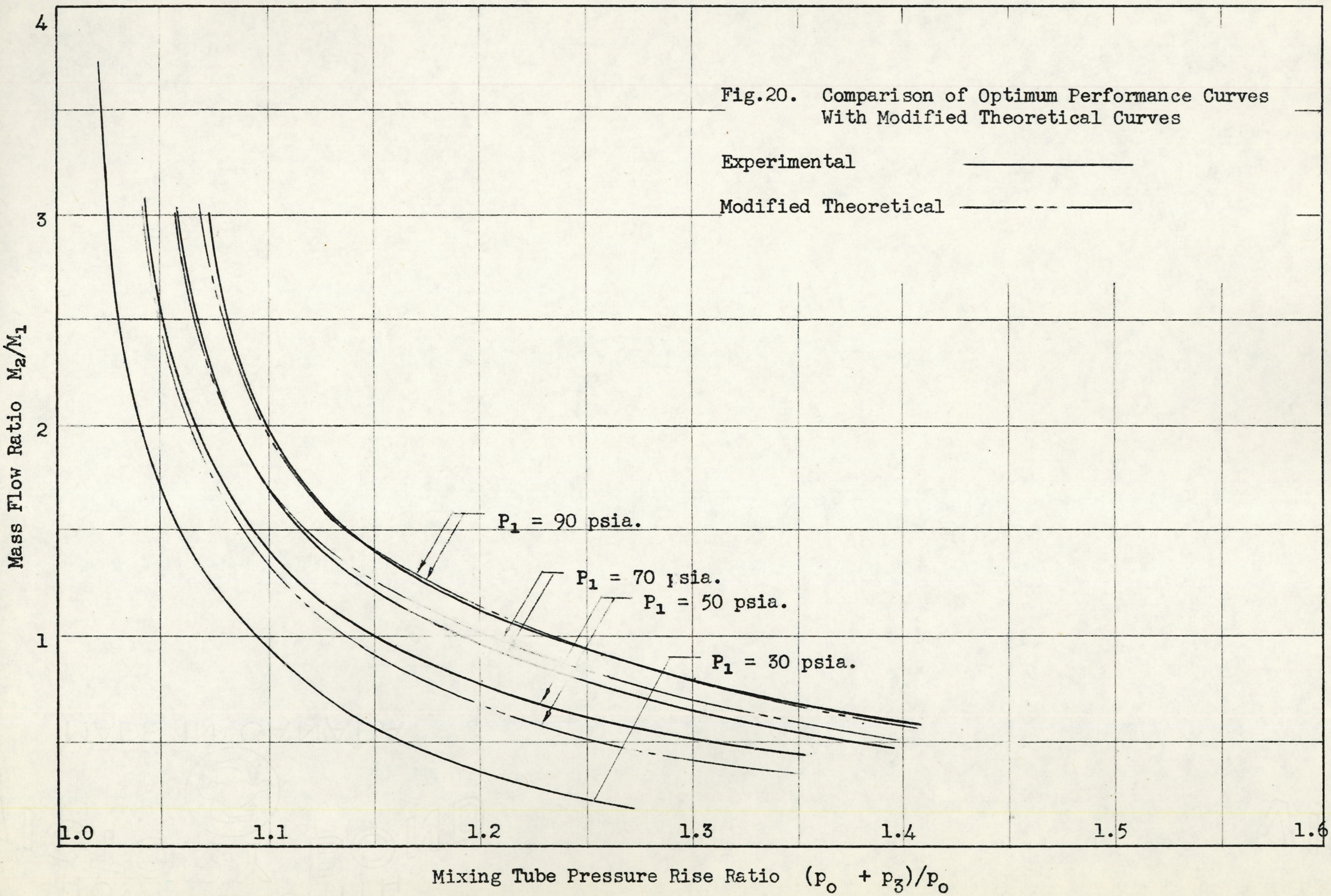

Fig.20. Comparison of Optimum Performance Curves With Modified Theoretical Curves

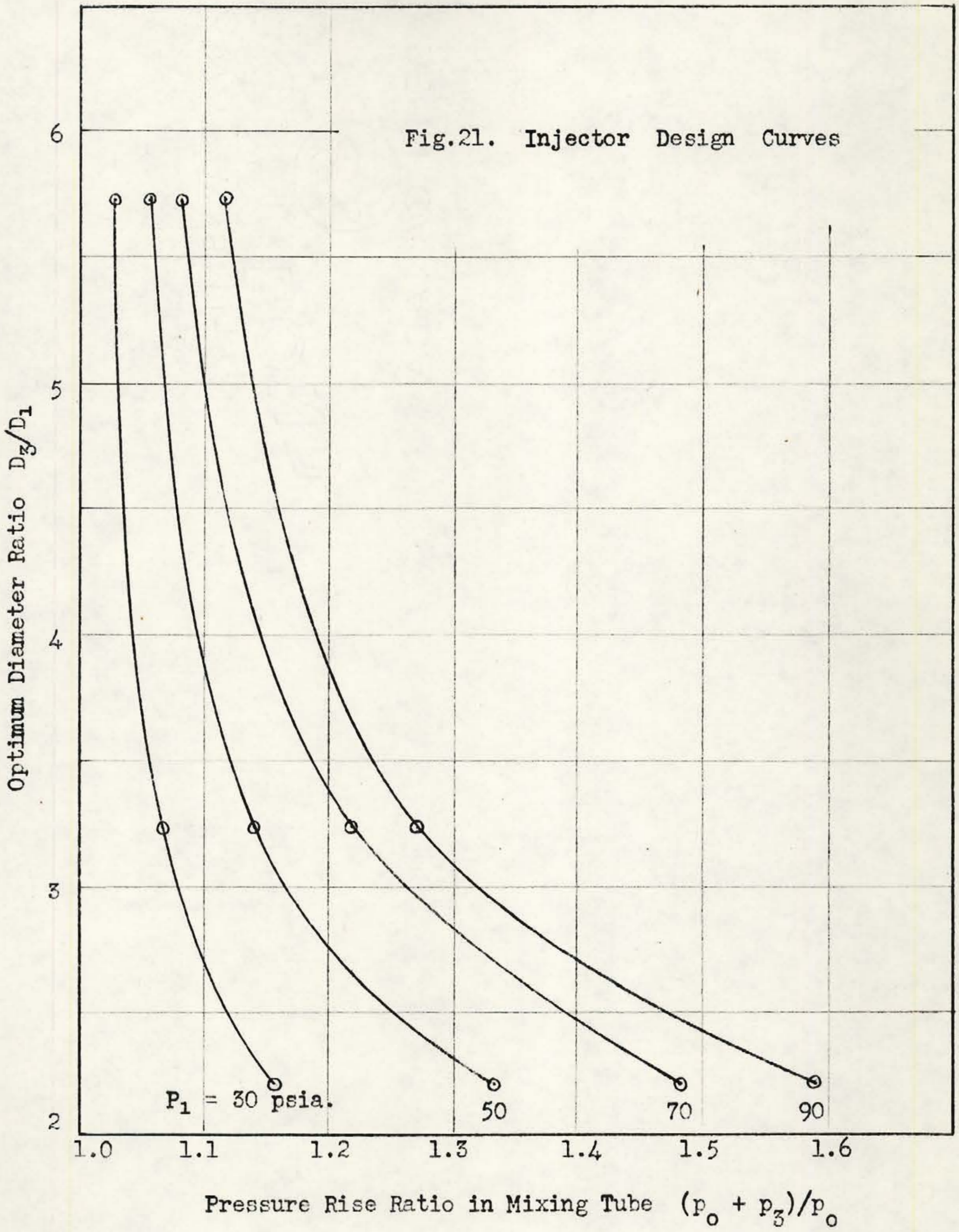
Fig.21. Injector Design Curves
Optimum Diameter Ratio D_3/D_1
6
5
4
3
2
P_1 = 30 psia.
50
70
90
1.0
1.1
1.2
1.3
1.4
1.5
1.6
Pressure Rise Ratio in Mixing Tube $(p_o + p_3)/p_o$

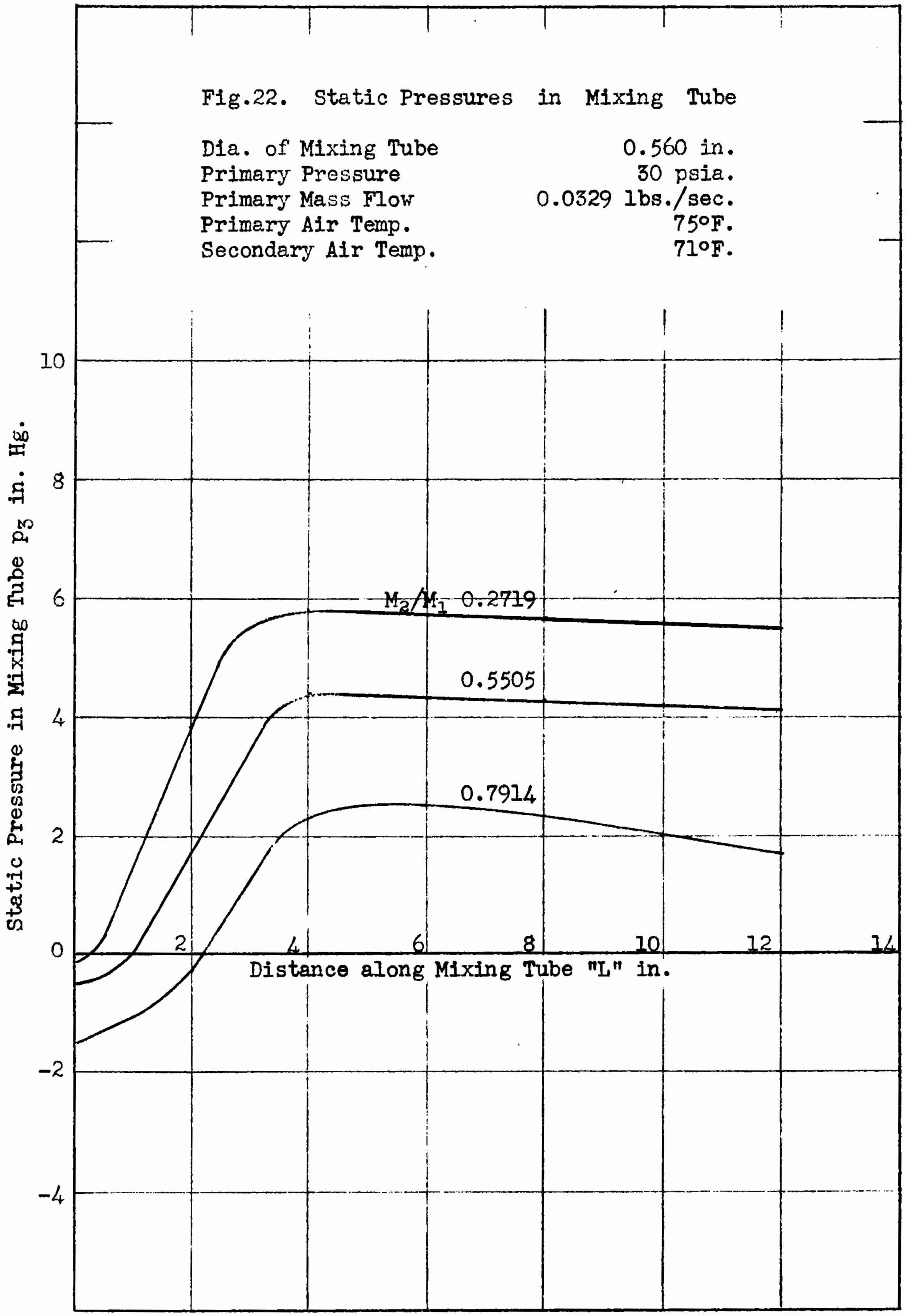

Fig.22. Static Pressures in Mixing Tube

Dia. of Mixing Tube	0.560 in.
Primary Pressure	30 psia.
Primary Mass Flow	0.0329 lbs./sec.
Primary Air Temp.	75°F.
Secondary Air Temp.	71°F.

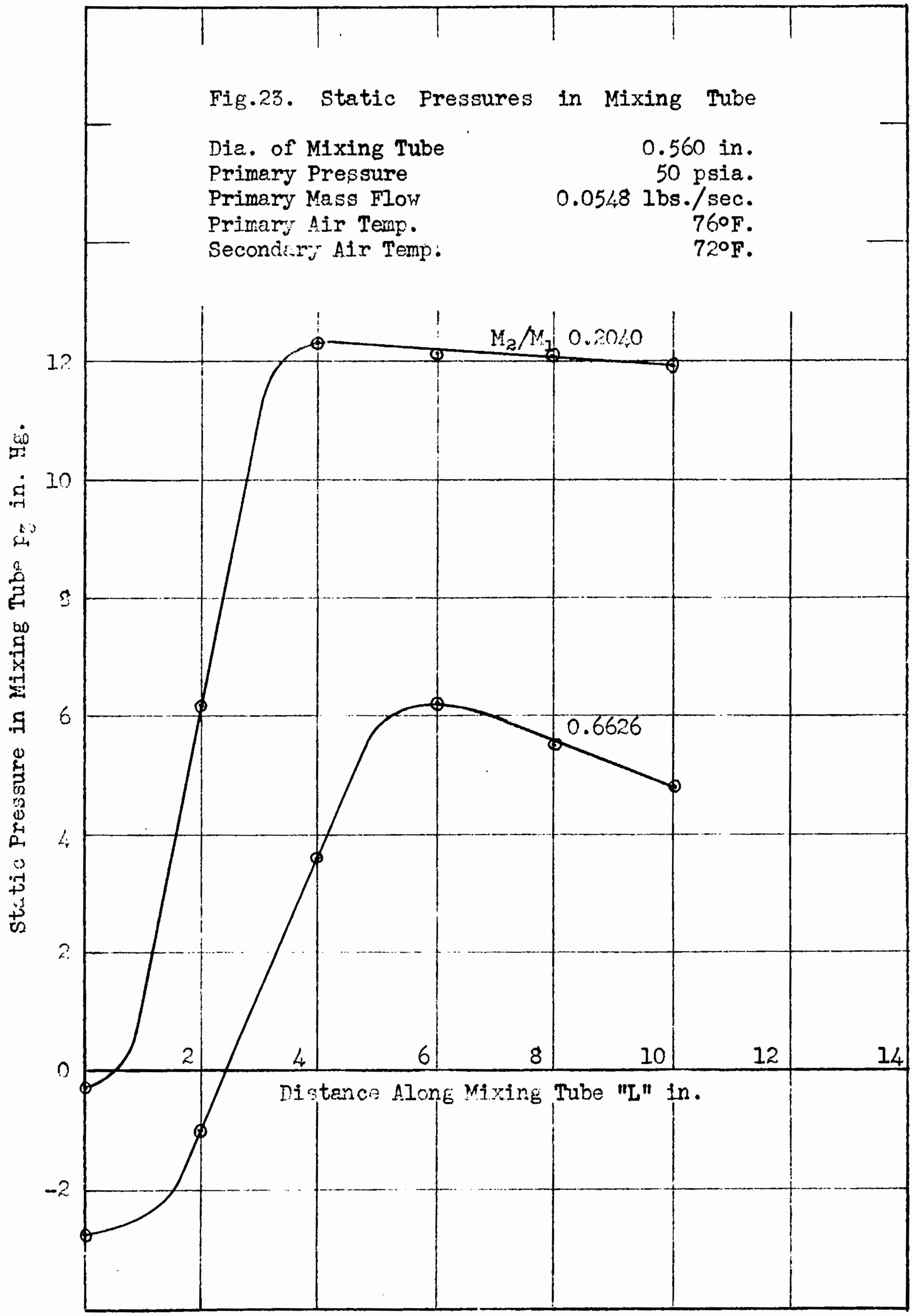

Fig.23. Static Pressures in Mixing Tube

Dia. of Mixing Tube	0.560 in.
Primary Pressure	50 psia.
Primary Mass Flow	0.0548 lbs./sec.
Primary Air Temp.	76°F.
Secondary Air Temp.	72°F.

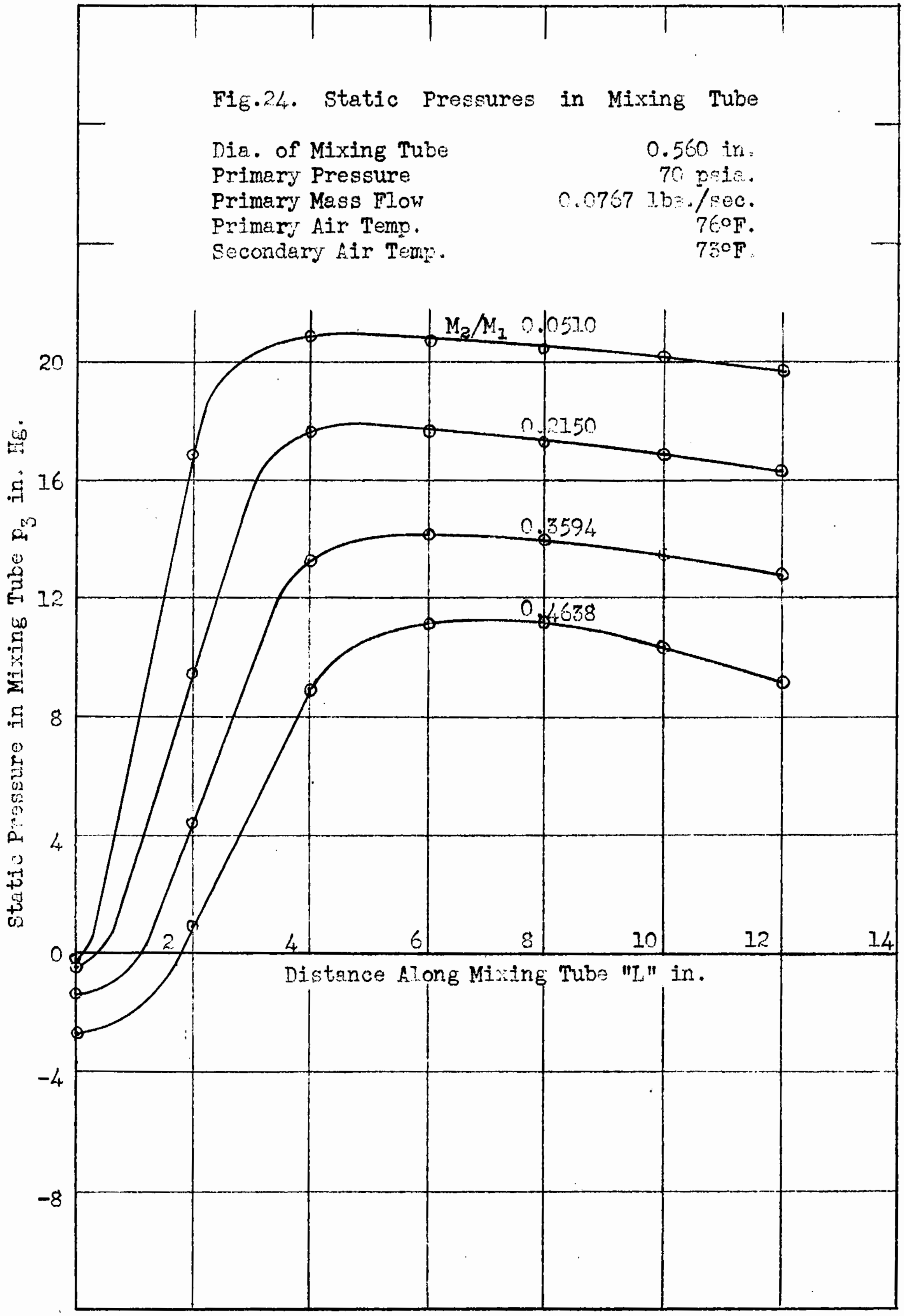

Fig.24. Static Pressures in Mixing Tube

Dia. of Mixing Tube	0.560 in.
Primary Pressure	70 psia.
Primary Mass Flow	0.0767 lbs./sec.
Primary Air Temp.	76°F.
Secondary Air Temp.	73°F.

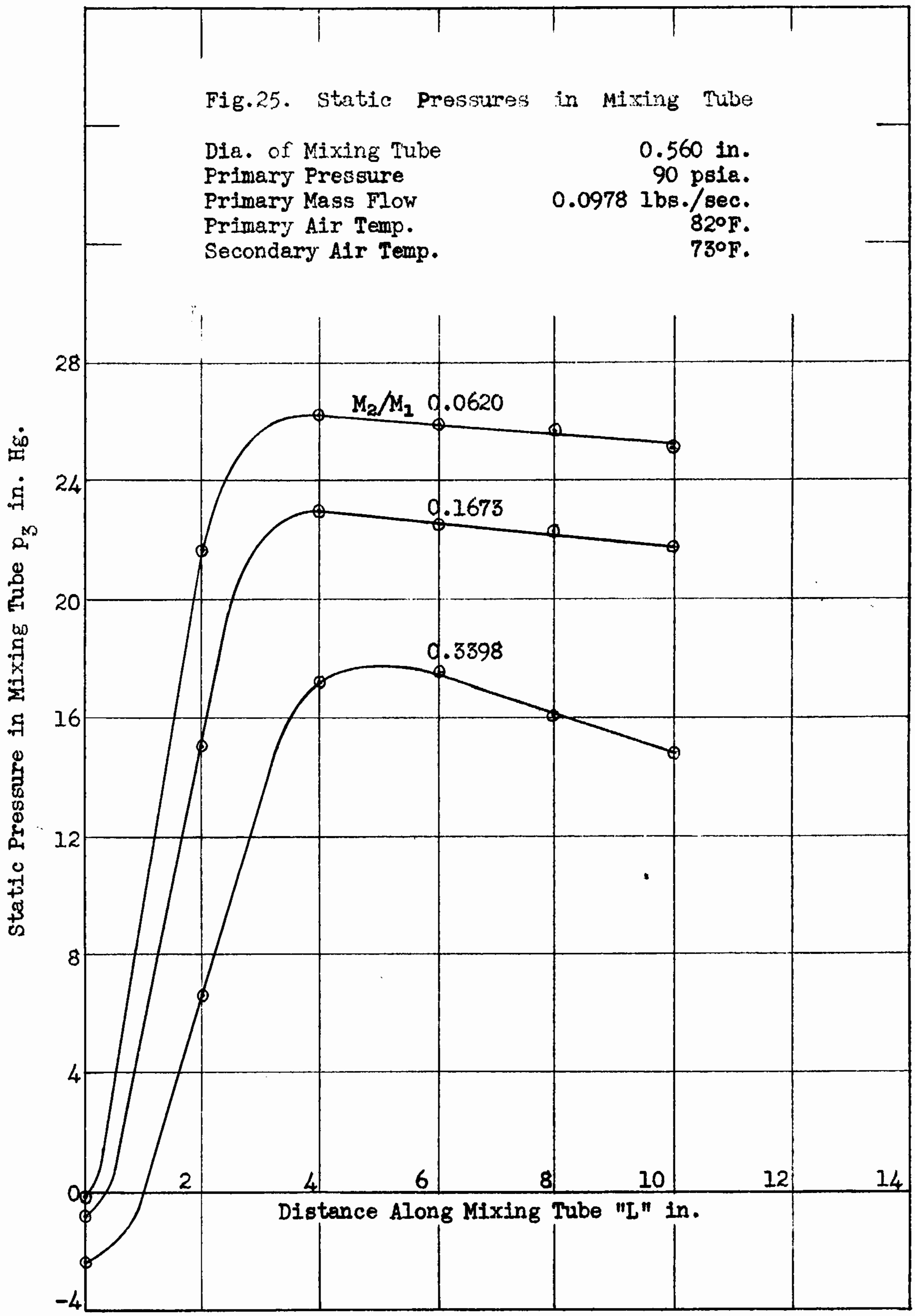
Fig.25. Static Pressures in Mixing Tube
Dia. of Mixing Tube 0.560 in.
Primary Pressure 90 psia.
Primary Mass Flow 0.0978 lbs./sec.
Primary Air Temp. 82°F.
Secondary Air Temp. 73°F.
M2/M1 0.0620
0.1673
0.3398
28
24
20
16
12
8
4
0
-4
2
4
6
8
10
12
14
Static Pressure in Mixing Tube p3 in. Hg.
Distance Along Mixing Tube "L" in.

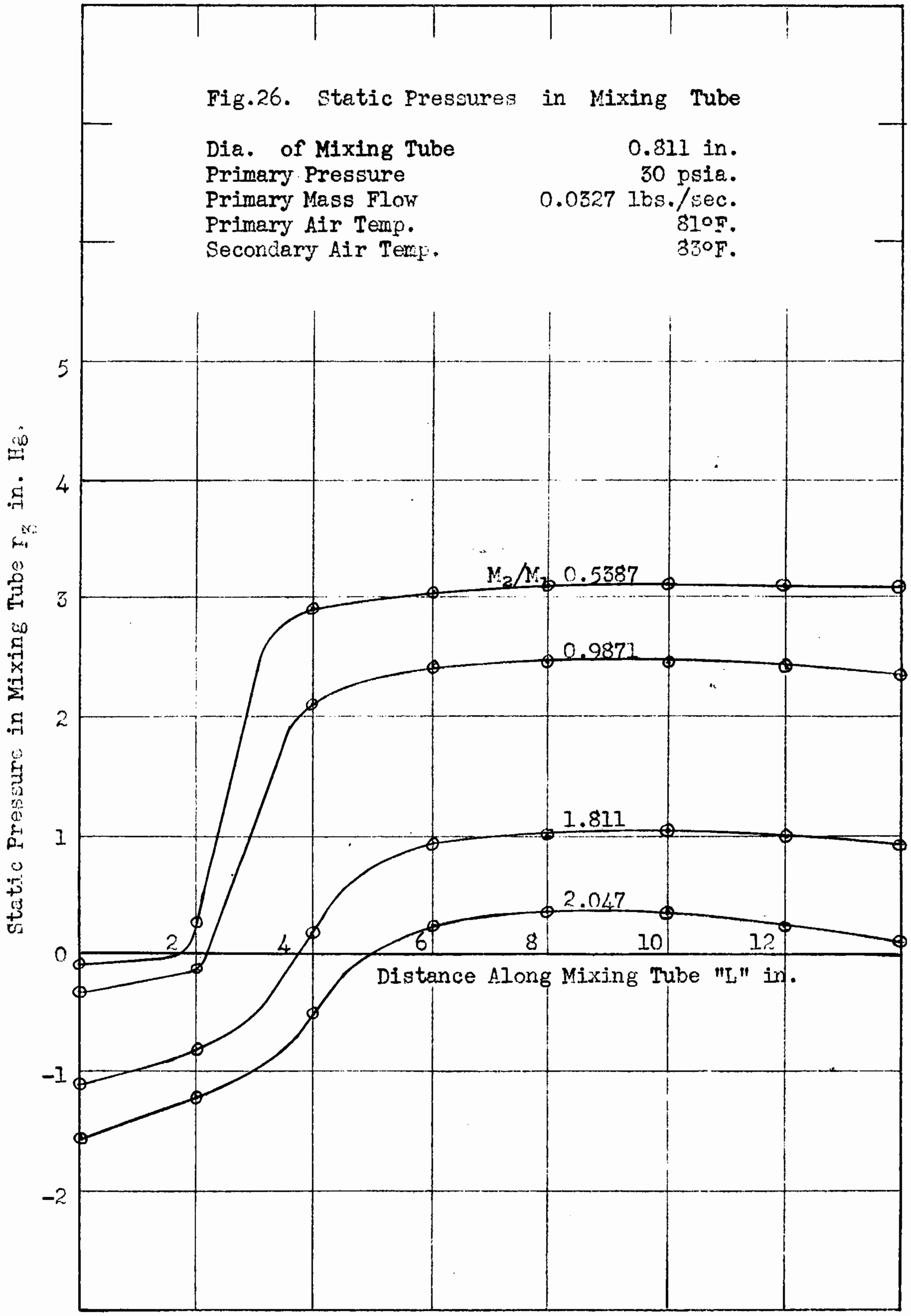
Fig.26. Static Pressures in Mixing Tube
Dia. of Mixing Tube 0.811 in.
Primary Pressure 30 psia.
Primary Mass Flow 0.0327 lbs./sec.
Primary Air Temp. 81°F.
Secondary Air Temp. 83°F.
M_2/M_1 0.5387
0.9871
1.811
2.047
Static Pressure in Mixing Tube P_x in. Hg.
Distance Along Mixing Tube "L" in.
5
4
3
2
1
0
-1
-2
2
4
6
8
10
12

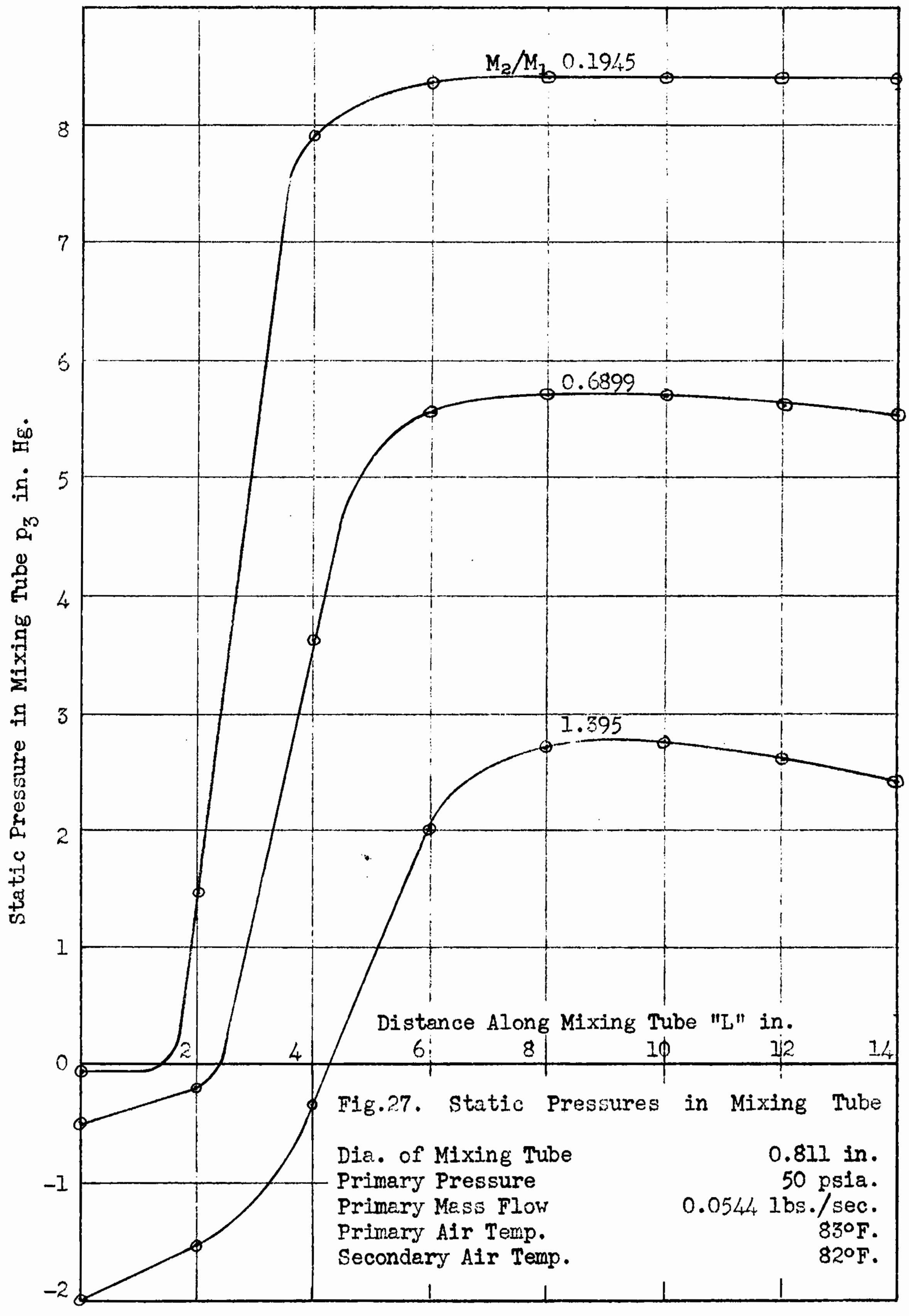

Fig.27. Static Pressures in Mixing Tube

Dia. of Mixing Tube	0.811 in.
Primary Pressure	50 psia.
Primary Mass Flow	0.0544 lbs./sec.
Primary Air Temp.	83°F.
Secondary Air Temp.	82°F.

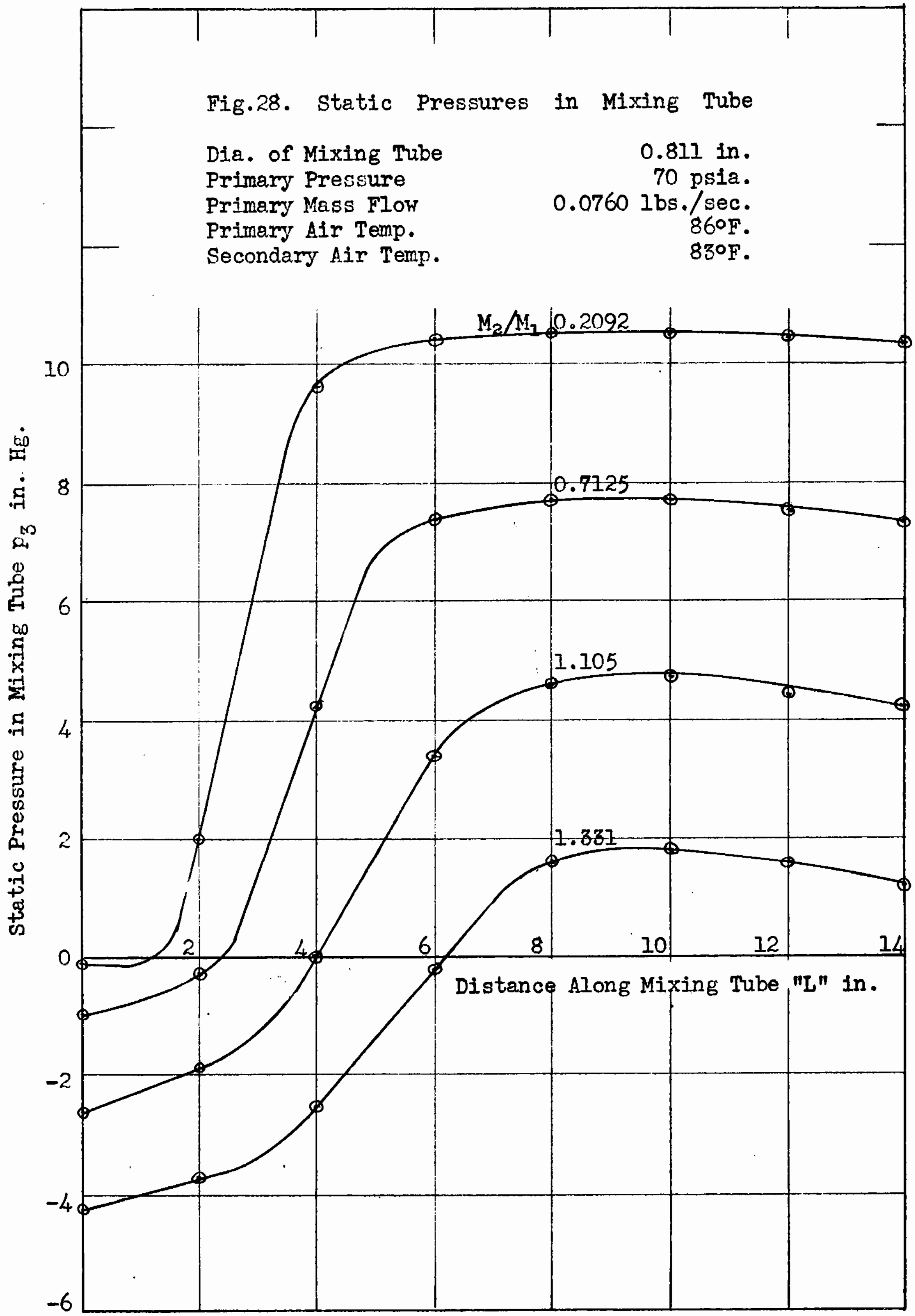
Fig.28. Static Pressures in Mixing Tube
Dia. of Mixing Tube 0.811 in.
Primary Pressure 70 psia.
Primary Mass Flow 0.0760 lbs./sec.
Primary Air Temp. 86°F.
Secondary Air Temp. 83°F.
M2/M1 0.2092
0.7125
1.105
1.331
Static Pressure in Mixing Tube p3 in. Hg.
10
8
6
4
2
0
-2
-4
-6
2
4
6
8
10
12
14
Distance Along Mixing Tube "L" in.

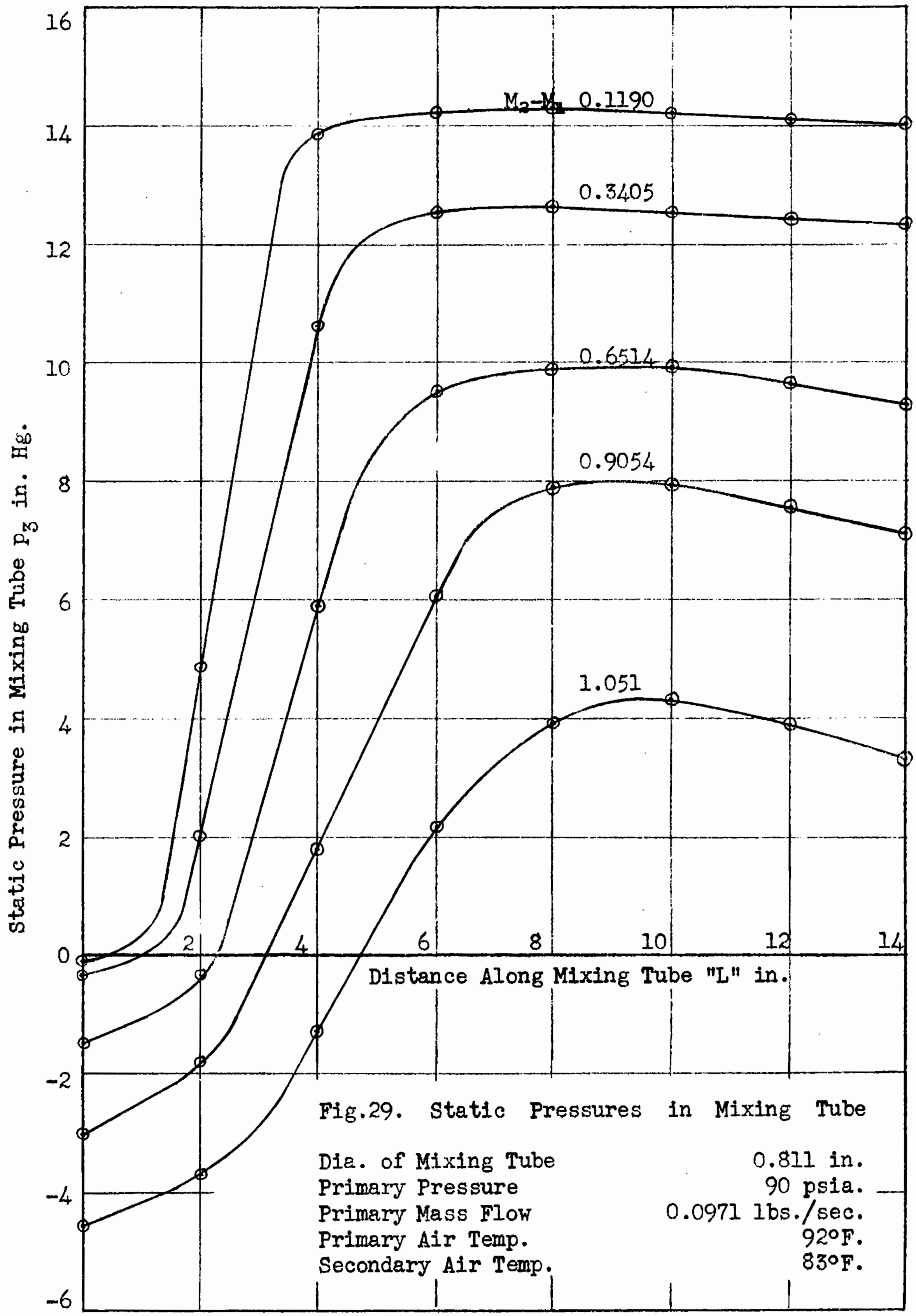

Fig.29. Static Pressures in Mixing Tube

Dia. of Mixing Tube	0.811 in.
Primary Pressure	90 psia.
Primary Mass Flow	0.0971 lbs./sec.
Primary Air Temp.	92°F.
Secondary Air Temp.	83°F.

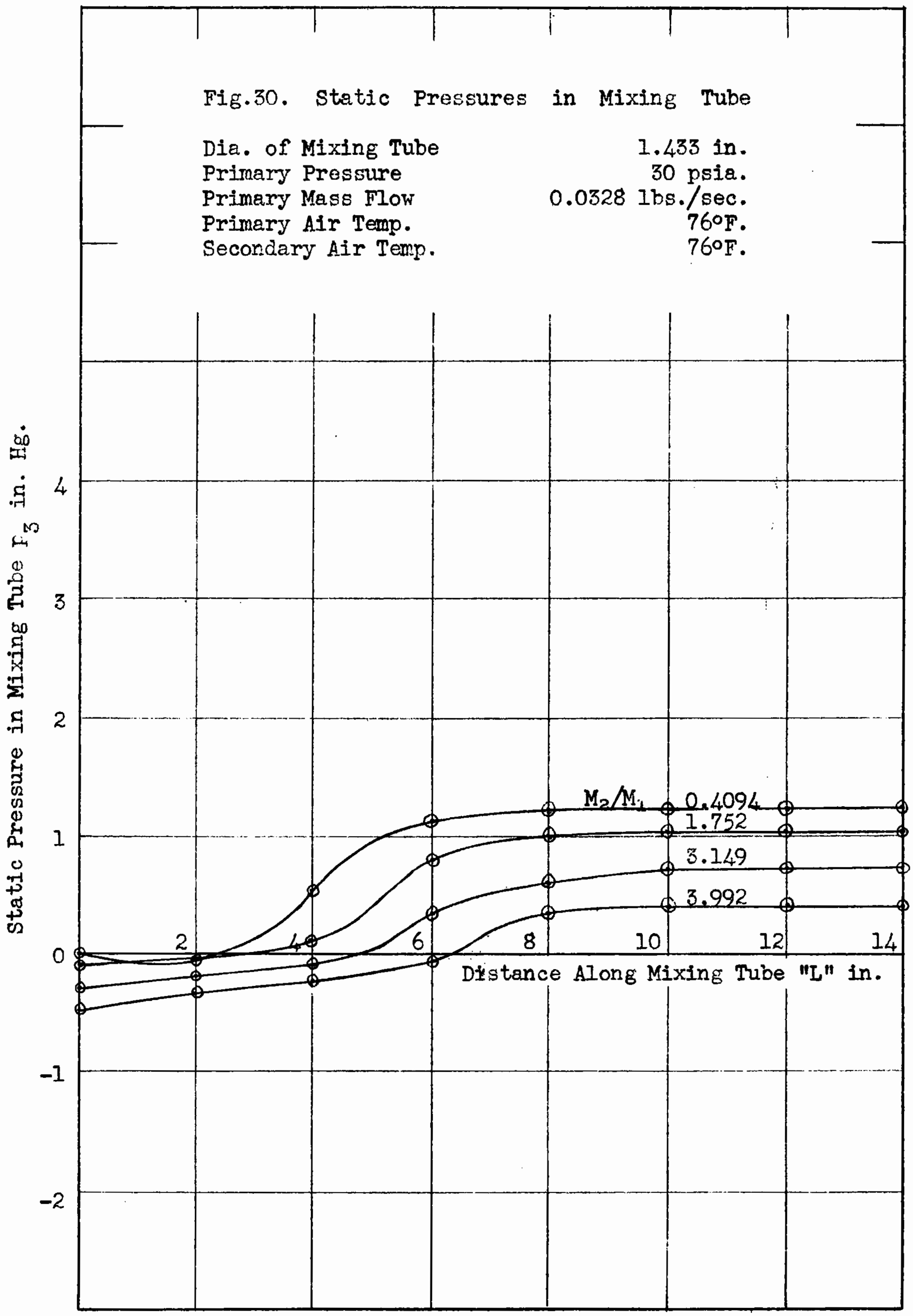
Fig.30. Static Pressures in Mixing Tube
Dia. of Mixing Tube 1.433 in.
Primary Pressure 30 psia.
Primary Mass Flow 0.0328 lbs./sec.
Primary Air Temp. 76°F.
Secondary Air Temp. 76°F.
Static Pressure in Mixing Tube P3 in. Hg.
Distance Along Mixing Tube "L" in.
M2/M1
0.4094
1.752
3.149
3.992
4
3
2
1
0
-1
-2
2
4
6
8
10
12
14

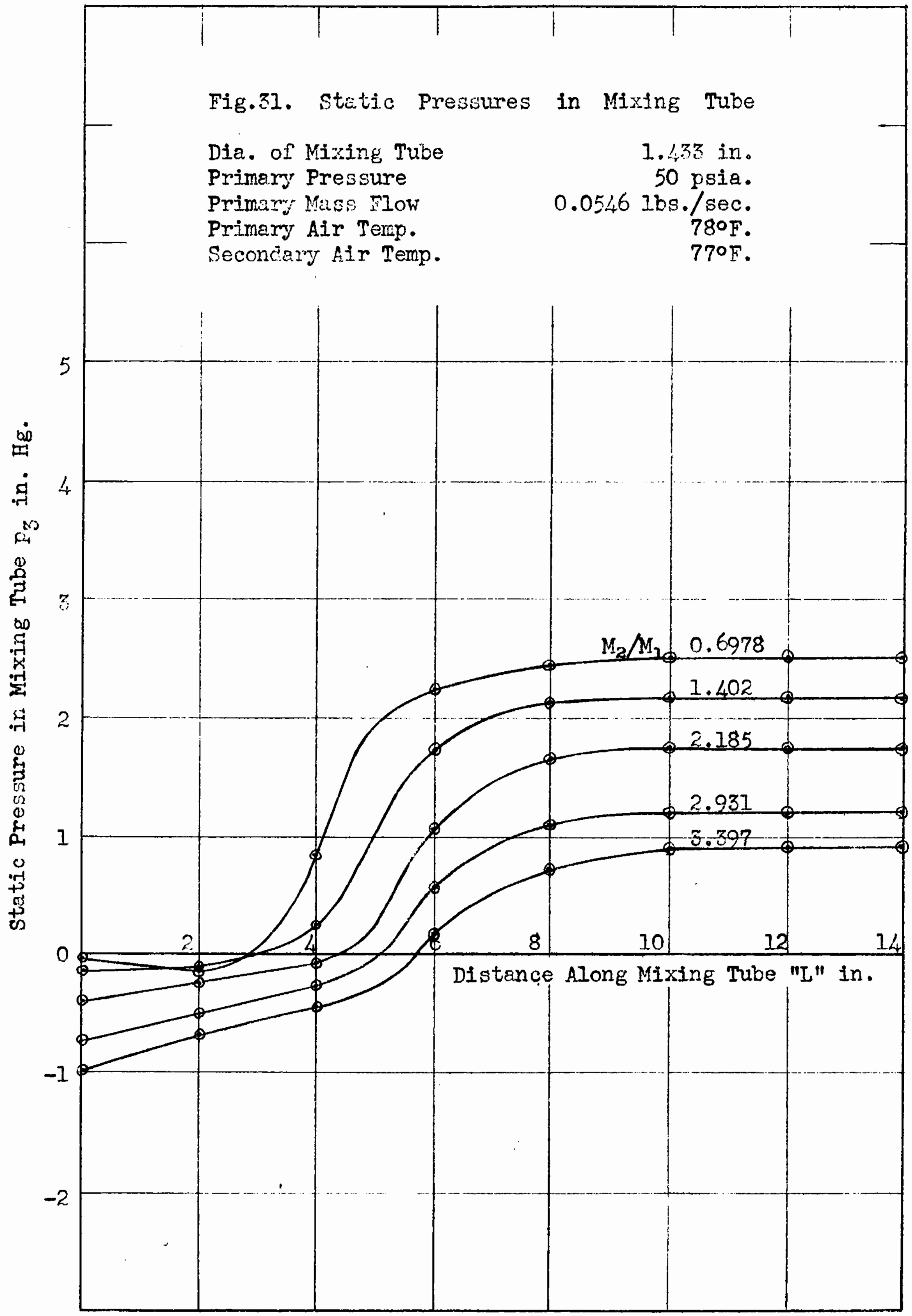
Fig.31. Static Pressures in Mixing Tube
Dia. of Mixing Tube 1.433 in.
Primary Pressure 50 psia.
Primary Mass Flow 0.0546 lbs./sec.
Primary Air Temp. 78°F.
Secondary Air Temp. 77°F.
M2/M1 0.6978
1.402
2.185
2.931
3.397
Static Pressure in Mixing Tube P3 in. Hg.
Distance Along Mixing Tube "L" in.
5
4
3
2
1
0
-1
-2
2
4
6
8
10
12
14

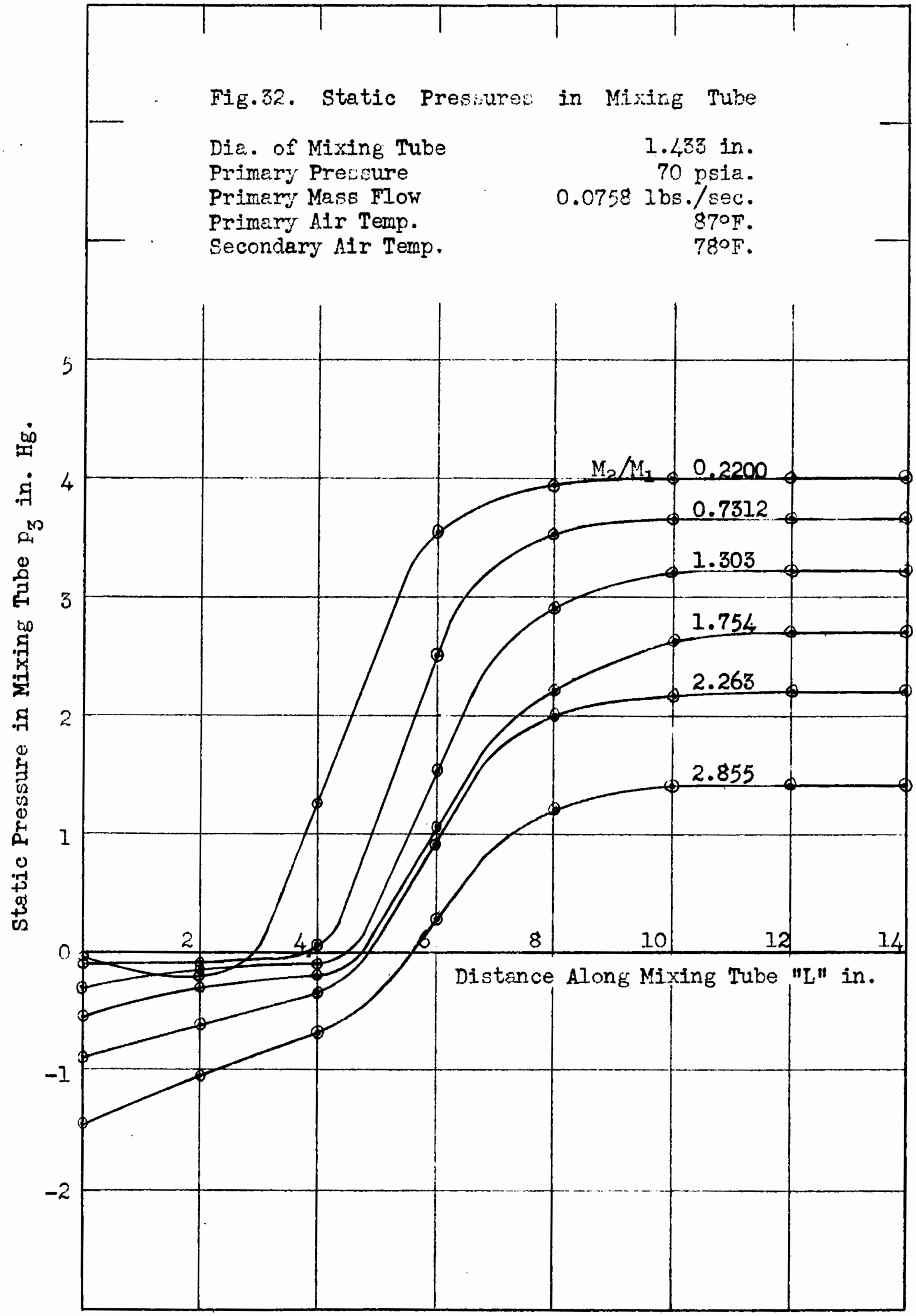

Fig.32. Static Pressures in Mixing Tube

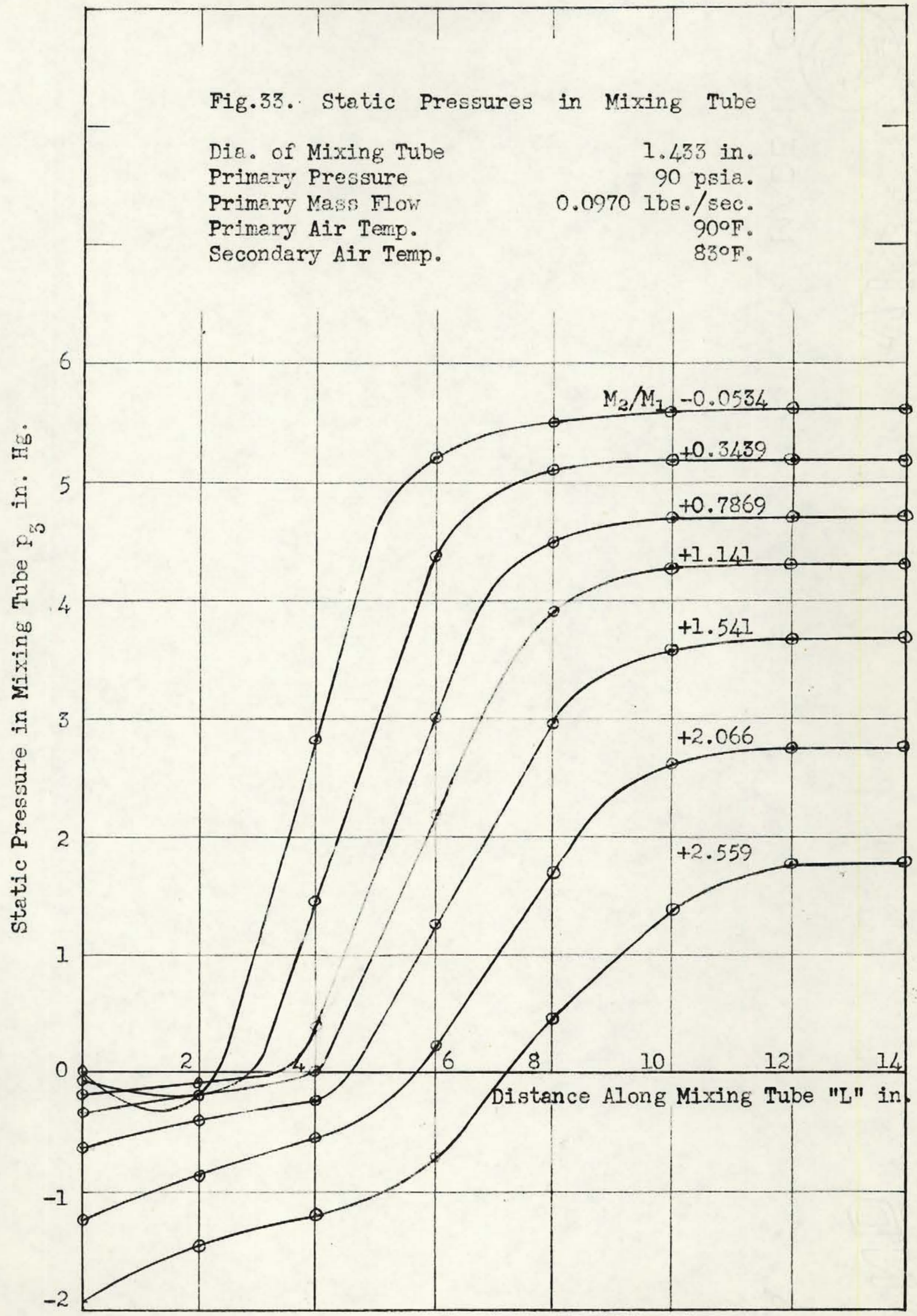

Fig.33. Static Pressures in Mixing Tube
Dia. of Mixing Tube 1.433 in.
Primary Pressure 90 psia.
Primary Mass Flow 0.0970 lbs./sec.
Primary Air Temp. 90°F.
Secondary Air Temp. 83°F.
M2/M1 -0.0534
+0.3439
+0.7869
+1.141
+1.541
+2.066
+2.559
Static Pressure in Mixing Tube p3 in. Hg.
Distance Along Mixing Tube "L" in.
6
5
4
3
2
1
0
-1
-2
2
4
6
8
10
12
14

BIBLIOGRAPHY

1. Charyk, J.J. : Investigation of Ejector Performance and the Mixing of Supersonic and Subsonic Fluid Streams. Project Squid Annual Program Report. January 1, 1950.

2. Diederichs, H., and Andrae, W.C. : Experimental Mechanical Engineering. John Wiley and Sons Inc., New York. 1930.

3. Ellerbrock, H.H. Jr. : General Treatment of Compressible Flow in Ejectors and Example of its Application to Problem of Effect of Ejector Addition on Thrust of Jet-Propulsion Units. N.A.C.A. Research Memorandum RM No. L6L23. 1947.

4. Flügel, G. : The Design of Jet Pumps. N.A.C.A. Technical Memorandum No. 982. 1941.

5. Goff, J.A., and Coogan, C.H. : Some Two Dimensional Aspects of the Ejector Problem. A.S.M.E. Transactions, Vol. 64. 1942.

6. Goldstein, S. : Modern Developments in Fluid Dynamics. Oxford Clarendon Press. 1938.

7. Jamison, R.R., and Mordell D.L. : The Compressible Flow of Fluids in Ducts. R. and M. No. 2031, A.R.C. Technical Report. 1945.

8. Keenan, J.H., and Neumann, E.P.: A Simple Air Injector. A.S.M.E. Transactions, Vol. 64. 1942.

9. Keuthe, A.M. : Investigations of the Turbulent Mixing Regions Formed by Jets. A.S.M.E. Vol. 57. 1935.

10. Lane, A.G. : A Study of the Air Ejector. McGill Masters Thesis. August 1950.

11. Liepmann, H.W., and Puckett, A.E. : Introduction to Aerodynamics of a Compressible Fluid. J. Wiley and Sons Inc., New York. 1947.

12. Prandtl, L. : Essentials of Fluid Dynamics. Blackie and Son Ltd., London. 1952.

13. Schlichting, H. : Boundary Layer Theory, Part I - Laminar Flows, Part II - Turbulent Flows. N.A.C.A. Technical Memorandum No. 1218. 1949.

14. Stodola, A. : Steam and Gas Turbines, Vol. 2. McGraw-Hill Book Co., Inc. 1927.

15. Streeter, V.L. : Fluid Dynamics. McGraw-Hill Book Co., Inc. 1948.

16. Szczeniowski, B. : Theory of the Jet Syphon. N.A.C.A. Technical Note 3385. 1955.

17. Turner, L.R., Addie, A.N., and Zimmerman, R.H. : Charts for the Analysis of One-Dimensional Steady Compressible Flow. N.A.C.A. Technical Note No. 1419. 1948.

18. Wilsted, H.D., Huddleston, S.C., and Ellis, C.W. : Effect of Temperature on Performance of Several Ejector Configurations. N.A.C.A. Research Memorandum, RM E9E16. 1949.

APPENDIX I

I - Formulae for Calculating Primary and Total Air Flows.

$$M_1 = 0.02535 \frac{P_e}{\sqrt{T_e}} \quad \ldots\ldots\ldots\ldots\ldots\ldots\ldots\ldots \quad (1)$$

where P_e = pressure upstream of primary nozzle psia.
T_e = Temp. upstream of primary nozzle °R.
(Nozzle diameter 0.25 in.)

$$(M_1 + M_2) = 0.0748 \sqrt{\frac{(\Delta P + B)\Delta P}{T_4}} \quad \ldots\ldots\ldots\ldots \quad (2)$$

where ΔP = Pressure in metering tank in. Hg.
B = Barometric pressure in. Hg.
T_4 = Temperature in metering tank °R.
(Orifice diameter 1.999 in.)

II - Theoretical Adiabatic Flow Equations Relating Pressure Ratio to Other Parameters.

$$\frac{u}{\sqrt{gRT}} = \sqrt{\frac{2\gamma}{\gamma - 1}\left[1 - \left(\frac{p}{P}\right)^{\frac{\gamma-1}{\gamma}}\right]} \quad \ldots\ldots\ldots\ldots \quad (3)$$

$$\frac{PA}{M\sqrt{gRT}} = \frac{\left(\frac{p}{P}\right)^{\frac{1}{\gamma}}}{\sqrt{\frac{2\gamma}{\gamma - 1}\left[1 - \left(\frac{p}{P}\right)^{\frac{\gamma-1}{\gamma}}\right]}} \quad \ldots\ldots\ldots\ldots \quad (4)$$

$$\frac{pA}{M\sqrt{gRT}} = \frac{\left(\frac{p}{P}\right)^{\frac{\gamma-1}{\gamma}}}{\frac{2\gamma}{\gamma-1}\left[1 - \left(\frac{p}{P}\right)^{\frac{\gamma-1}{\gamma}}\right]} \quad \ldots\ldots\ldots\ldots \quad (5)$$